

UNIVERSITI MALAYSIA PAHANG

BORANG PENGESAHAN STATUS TESIS*

JUDUL: ACTIVE SWAY CONTROL OF A GANTRY CRANE USING HYBRID INPUT-SHAPING AND PID CONTROL SCHEMES

SESI PENGAJIAN: 2011/2012

Saya LATIFAH BINTI SHABUDIN (860426-35-5184)
(HURUF BESAR)

mengaku membenarkan tesis (Sarjana Muda/Sarjana /Doktor-Falsafah)* ini disimpan di Perpustakaan dengan syarat-syarat kegunaan seperti berikut:

1. Tesis adalah hakmilik Universiti Malaysia Pahang (UMP).
2. Perpustakaan dibenarkan membuat salinan untuk tujuan pengajian sahaja.
3. Perpustakaan dibenarkan membuat salinan tesis ini sebagai bahan pertukaran antara institusi pengajian tinggi.
4. **Sila tandakan (√)

SULIT

(Mengandungi maklumat yang berdarjah keselamatan atau kepentingan Malaysia seperti yang termaktub di dalam AKTA RAHSIA RASMI 1972)

TERHAD

(Mengandungi maklumat TERHAD yang telah ditentukan oleh organisasi/badan di mana penyelidikan dijalankan)

TIDAK TERHAD

Disahkan oleh:



(TANDATANGAN PENULIS)



(TANDATANGAN PENYELIA)

Alamat Tetap:

BLOCK C-1-08 TAMAN HAJI MOHD AMIN
PERMATANG PAUH, 13500
PULAU PINANG

MOHD ZAIDI B. MOHD TUMARI
(Nama Penyelia)

Tarikh : 21 JUNE 2012

Tarikh : 21 JUNE 2012

CATATAN:

- * Potong yang tidak berkenaan.
- ** Jika tesis ini SULIT atau TERHAD, sila lampirkan surat daripada pihak berkuasa/organisasi berkenaan dengan menyatakan sekali tempoh tesis ini perlu dikelaskan sebagai atau TERHAD.
- ◆ Tesis dimaksudkan sebagai tesis bagi Ijazah doktor Falsafah dan Sarjana secara Penyelidikan, atau disertasi bagi pengajian secara kerja kursus dan penyelidikan, atau Laporan Projek Sarjana Muda (PSM).

ACTIVE SWAY CONTROL
SHAP



USING HYBRID INPUT
IES

LATIFAH BINTI SHABUDIN

This thesis is submitted as partial fulfilment of the requirements for the award of the Bachelor of
Electrical Engineering (Electronics)

Faculty of Electrical & Electronic Engineering
University Malaysia Pahang

June 2012

“I hereby acknowledge that the scope and quality of this thesis is qualified for the award of the Bachelor of Electrical Engineering (Electronics)”

Signature: 

Name: MOHD ZAIDI BIN MOHD TUMARI

Date: 21st JUNE 2012

“All the trademark and copyrights use herein are property of their respective owner. References of information from other sources are quoted accordingly; otherwise the information presented in this report is solely work of the author.”

Signature :  _____

Author : LATIFAH BT SHABUDIN

Date : 21 JUNE 2012

*Specially dedicated to my family
To My Beloved Mother and Dad, My brother and sister, My Aunty & My
Grandmother and those people who have guided and inspired me throughout my
journey of education.*

Thank's For Everything...

ACKNOWLEDGEMENT

In preparing this thesis, I was in contact with many people, researchers, academicians and practitioners. They have contributed towards my understanding and thoughts. In particular, I wish to express my sincere appreciation to my supervisor, Mr. Mohd Zaidi B. Mohd Tumari, for encouragement, guidance, critics, friendship, advice, information and motivation. Without their continued support and interest, this thesis would not have been the same as presented here.

I am also indebted to Universiti Malaysia Pahang (UMP) for funding my degree study. Librarians at UMP also deserve special thanks for their assistance in supplying the relevant literatures and guiding me in using e-journal.

My sincere appreciation also extends to all my colleagues, and others who have provided assistance at various occasions. Their views and tips are useful indeed. Unfortunately, it is not possible to list all of them in this limited space. I am grateful to all my family members for their moral support, advice and understanding me.

Thank you

ABSTRACT

The idea of this project presents investigations into the development of hybrid input-shaping and PID control schemes for active sway control of a gantry crane system. The main purpose of controlling a gantry crane is transporting the load as fast as possible without causing any excessive sway at the final destination. However, most of the common gantry crane results in a sway motion when payload is suddenly stopped after a fast motion. The failure of controlling crane also might cause accident and may harm people and the surrounding. The application of positive input shaping involves a technique that can reduce the sway by creating a common signal that cancels its own vibration and it also will be used as a feed-forward control which is for controlling to sway angle of the pendulum, while the proportional integral derivative (PID) controller will be used as a feedback control which is for controlling the crane position. The modeling of gantry crane will be used to simulate the system using MATLAB software. The ready-made gantry crane hardware system will be used for real-time experiment. The simulation result will be compare with experiment result. Finally, a comparative assessment of the control techniques is presented and discussed.

ABSTRAK

Tujuan utama projek ini dilaksanakan, adalah untuk mengawal pergerakan ayunan bagi sistem kren gantry, menggunakan hasil gabungan dua teknik yang berbeza iaitu pembentukan input positif dan sistem kawalan PID. Faktor utama mengawal kren gantri adalah untuk memastikan kren dapat mengangkat beban secepat mungkin dan meletakkan beban tepat pada kawasan yang dikehendaki tanpa belaku sebarang ayunan. Walau bagaimanapun, kebiasaannya kebanyakan kren gantri akan berayun apabila muatan yang dibawa berhenti secara pantas. Kegagalan mengawal pergerakan kren juga mungkin menyebabkan kemalangan dan boleh memudaratkan orang ramai dan keadaan sekitarnya. Oleh itu, kaedah pembentukan input positif diperkenalkan bagi mengurangkan ayunan pergerakan kren dengan mewujudkan isyarat biasa yang mampu menghilangkan kadar getaran kren tersebut, selain itu ia juga akan digunakan sebagai kawalan suapan hadapan bertujuan untuk mengawal dan mempengaruhi sudut bandul, manakala sistem kawalan PID akan digunakan sebagai kawalan maklum balas untuk mengawal kedudukan kren. Pemodelan kren gantri akan digunakan dan diterjemahkan ke dalam perisian MATLAB. Hasil keputusan dari perisian MATLAB yang diperolehi akan dibandingkan dengan hasil eksperimen. Akhir sekali, keputusan penilaian perbandingan teknik-teknik kawalan ini dibentangkan dan dibincangkan.

TABLE OF CONTENTS

CHAPTER	TITLE	PAGE
	TITLE	i
	DECLARATION	ii
	DEDICATION	iii
	ACKNOWLEDGEMENT	iv
	ABSTRACT	v
	ABSTRAK	vi
	TABLE OF CONTENT	vii
	LIST OF TABLES	x
	LIST OF FIGURES	xi
	LIST OF SYMBOL	xiv
	LIST OF APPENDICES	xv
1	INTRODUCTION	1
	1.1 Overview	1
	1.2 Problem Statement	2
	1.3 Objective	3
	1.4 Scope of Project	3
	1.5 Dissertation Organization	4
2	LITERATURE REVIEW	5
	2.1 An Overview	5
3	METHODOLOGY	10
	3.1 Introduction	10

3.2	Modeling of gantry crane	12
3.2.1	Specifications of the lab-scale gantry crane	13
3.2.2	Dynamic modeling of gantry crane	14
3.2.3	State space representation of the system	15
3.2.4	Parameter used in this dynamical equation	16
3.3	Research on positive input shaping techniques	16
3.3.1	Objective Input Shaping	16
3.3.2	Operation of Input Shaping	17
3.3.3	Bang-bang Input Techniques	18
3.3.4	Development of positive input shaping	18
3.3.5	Design equation of Input Shaping Schemes	19
3.3.6	Advantages of Input Shaping	21
3.4	Research on PID controller techniques	21
3.4.1	Objective PID control	21
3.4.2	Combinational of all three modes (P, I and D)	22
3.4.3	PID control procedures in closed loop system	23
3.4.4	Characteristics of PID	25
3.4.5	Ziegler–Nichols Frequency Response Method	29
3.5	Simulation Studies	31
3.6	Experimental Studies	35
3.6.1	Verification of Control Design	35
3.6.2	Data Collection and Analysis Controller Design	39
4	RESULT AND DISCUSSION	42
4.1	Introduction	42
4.2	Comparative Assessment of Simulation	43
4.3	Simulation result using MATLAB software	43
4.3.1	Simulation result without controller	44
4.3.2	Determination of Cut-off Frequency	47
4.3.3	The Unshaped Bang – Bang Torque Input Design	48

4.4	Simulation result with controller based on hybrid input shaping and PID control schemes	50
4.4.1	Positive Zero Derivative (PZS) and PID Controller schemes	50
4.4.2	Positive Zero Derivative (PZSD) and PID Controller schemes	52
4.4.3	Positive Zero Derivative-derivative (PZSDD) and PID Controller schemes	54
4.5	Comparison in Simulation Result	56
4.5.1	Comparison of Power Spectra Density	56
4.5.2	Comparison of Sway Angle of the Pendulum	58
4.5.3	Comparison of Horizontal Position Cart	61
4.6	Experiment results using CEM-Tools	65
4.6.1	Experiment result without controller	66
4.6.2	Bang – Bang Torque Input Design	67
4.6.3	Experiment result with controller based on PID control schemes	69
4.7	Experimental Result Analysis	71
5	CONCLUSION AND RECOMMENDATION	73
5.1	Conclusion	73
5.2	Limitation of the Project	74
5.3	Recommendation	75
	REFERENCES	76
	APPENDICES	79
	Appendix A	79

LIST OF TABLES

TABLE NO.	TITLE	PAGE
3.1	Lab-scale gantry crane specifications	13
3.2	Positive Input Shaping Techniques	19
3.3	The characteristics of P, I, D controllers	25
3.4	Critical Gain (K_{cr}) and Critical Period (P_{cr})	29
3.5	Calculation of PID based on Ziegler	30
4.1	Response of Power Spectra Density after apply controller	57
4.2	Response of Swing Angle of Pendulum after apply controller	59
4.3	Level sway reduction of the single pendulum	60
4.4	Response of Horizontal position of the cart after apply controller	63
4.5	Specification of horizontal position of cart response	64
4.6	Level sway reduction of the single pendulum	71

LIST OF FIGURES

FIGURE NO.	TITLE	PAGE
1.1	Gantry Crane	1
3.1	Work Methodology	11
3.2	Gantry Crane Model	12
3.3	Gantry Crane Pendulum Hardware	13
3.4	Illustration of input shaping technique	17
3.5	Block diagram of input shaping outside closed loop system	17
3.6	Block Diagram of a PID Control	23
3.7	The PID controller structure	24
3.8	Plot of PV vs time, for three values of K_p	26
3.9	Plot of PV vs time, for three values of K_i	27
3.10	Plot of PV vs time, for three values of K_d	28
3.11	Step Response for Critical Period	29
3.12	Sustained oscillation response	30
3.13	Block diagram for hybrid input shaping and PID control schemes	31
3.14	Simulink Model of Gantry Crane System	32
3.15	Input shaping controller inside the system	32
3.16	PID controller inside the system	33
3.17	2D modeling of gantry crane inside the system	33
3.18	Source code modeling of state space	34
3.19	Block Parameter of Input Shaping	34
3.20	Parameter Setting for Step 1	36
3.21	Parameter Setting for Step 2	36
3.22	Parameter Setting for Step 3	37

3.23	Variable of Input Shaping in CEM-Tools	38
3.24	Configuration of workspace in CEM-Tools	38
3.25	SIM-Tool Initial Block Diagram	40
3.26	Model of gantry crane design without controller	40
3.27	Model of gantry crane design with controller	41
3.28	Interfacing connection between CEM-Tools and Gantry Crane Pendulum	41
4.1	A block diagram design of a gantry crane system in MATLAB	44
4.2	Power Spectra Density without Controller	45
4.3	Amplitude of sway angle of the pendulum	46
4.4	Horizontal position of the cart	46
4.5	Cut-off frequency	47
4.6	Bang-bang Input Torque for PZS	48
4.7	Bang-bang Input Torque for PZSD	49
4.8	Bang-bang Input Torque for PZSDD	49
4.9	Power Spectra Density PZS and PID	50
4.10	Amplitude of sway angle of the pendulum PZS and PID	51
4.11	Horizontal position of the cart PZS and PID	51
4.12	Power Spectra Density PZSD and PID	52
4.13	Amplitude of sway angle of the pendulum PZSD and PID	53
4.14	Horizontal position of the cart PZSD and PID	53
4.15	Power Spectra Density PZSDD and PID	54
4.16	Amplitude of sway angle of the pendulum PZSDD and PID	55
4.17	Horizontal position of the cart PZSDD and PID	55
4.18	Comparison of Power Spectra Density	56
4.19	Comparison response of sway angle of pendulum	58

4.20	Level of Sway Reduction	61
4.21	Comparison Response of Horizontal Position Cart	62
4.22	Comparison Times Response of the System	65
4.23	The horizontal position of cart and sway angle of the pendulum without controller	67
4.24	The horizontal position of cart and sway angle of the pendulum at $P=350$, $I=385$ and $D=90$	70
4.25	The horizontal position of cart and sway angle of the pendulum at $P=345$, $I=385$ and $D=84$	70
4.26	The horizontal position of cart and sway angle of the pendulum at $P=320$, $I=0.3$ and $D=15$	71
4.27	Comparison levels of sway reduction with and without controller	72

LIST OF SYMBOL

CEM-Tool	Computer-aided Engineering & Mathematics Tool
$e(t)$	Error signal
g	Gravity acceleration (m/s^2)
K_d	Derivative gain
K_i	Integral gain
K_p	Proportional gain
L	Length of rode (m)
M	Mass of the trolley (kg)
m	Mass of the load (kg)
PID	Proportional Integral Derivative
PZS	Positive Zero Sway
PZSD	Positive Zero Sway Derivative
PZSDD	Positive Zero Sway Derivative-Derivative
R	Difference between the desired input value
SIM-Tool	Simulation Tool
x	Horizontal position of cart
T_r	Rise Time
T_s	Settling Time
%OS	Percentages Overshoot
ω_n	Natural frequency

LIST OF APPENDIXES

APPENDIX	TITLE	PAGE
A	Coding MATLAB based on PZS, PZSD and PZSDD	79
i	Positive Zero Sway (PZS)	80
ii	Positive Zero Sway Derivative (PZSD)	82
iii	Positive Zero Sway Derivative-Derivative (PZSDD)	84

CHAPTER 1

INTRODUCTION

1.1 Overview

Cranes are commonly employed in the transport industry for the loading and unloading of freight, in the construction industry for the movement of materials and in the manufacturing industry for the assembly of heavy equipment. In addition crane is important as a lifting machine, generally equipped with wire ropes or chains and sheaves, which can be used to lift and lower materials vertically and horizontally as shown in Figure 1.1. It used one or more simple machines to create mechanical advantages and thus move loads beyond the capability of a human.



Figure 1.1: Gantry Crane

1.2 Problem statement

The requirement of precise cart position control of gantry crane implies that the residual sway of the system should be zero or near zero. Almost every industry uses a gantry crane for its material handling applications. These gantry cranes are mostly equipped with a cabled hoisting mechanism, which are prone to the load sway problems. Sway persists even if a skilled operator is operating the crane. Because of danger to the ground staff and ground equipment, these load sways can't be accepted for such material handling applications. Furthermore, another factor that must be considered is the effect of the load swing and disturbance on the load will risk hazard in material handling application of a gantry crane system. Thus, anti-swing control of material handling cranes is becoming a necessity day by day and many researchers for anti-sway system have been progressed for a long time after the first appearance of the crane.

Regarding on this matter, active sway control of the gantry crane need to be developed, this project will focus on developing hybrid input shaping and PID control schemes. The application of positive input shaping involves a technique that can reduce the sway by creating a common signal that cancels its own vibration and it also will be used as a feed-forward control which is for controlling to sway angle of the pendulum, while the Proportional Integral Derivative (PID) controller will be used as a feedback control which is for controlling the crane position. The design control model can be applied to Gantry Crane Pendulum System hardware to get the result based on the real experimental implementation.

1.3 Objectives

The objectives of this project are:

- i. To design positive input shaping techniques and PID controller for the anti-sway control of a gantry crane system.
- ii. To control and minimize the sway angle of gantry crane as fast as possible without causing any sway at the final position.
- iii. To compare the simulation results with experimental results.

1.4 Scope of Project

The scopes that need to be proposed for this project are:

- i. To study and understand the concept of input shaping and PID controller
- ii. Study the dynamic modeling of the Gantry Crane to design the input shaping algorithm.
- iii. Design PID controller based on Ziegler Nichols closed loop method
- iv. Design positive input shaping based on:
 - Positive zero sway (PZS)
 - Positive zero sway derivative (PZSD)
 - Positive zero sway derivative-derivative (PZSDD) shapers.
- v. Simulate the design using MATLAB
- vi. Do experiment by using Pendulum System Hardware.

1.5 Dissertation Organization

This thesis is a combination of five chapters that contains and elaborates specific topics such as the Introduction, Literature Review, Methodology, Result and Discussion, and Conclusion.

Chapter 1 basically introduced the background of the project. In this chapter, the background of project, problem statement, objectives and scope of the project will be discussed.

Chapter 2 contains the literature review of various technical papers, journals and researches regarding to the modeling and various anti sway techniques in controlling the excessive sway of a gantry crane.

Chapter 3 will be focused on methodologies for the development of hybrid input-shaping and PID control schemes for anti-sway control of a gantry crane system. Each step in the work methodology will be explained.

Chapter 4 will be focused on the simulation and experiment result and discussion of MATLAB and CEM-Tools software. Comparison between each positive input shaping derivative order with PID controller as a feedback has been developed. This chapter also discusses a performance of each order and which orders are more efficient to reduce sway angle of the pendulum base on the experimental results.

Chapter 5 will be focused an overall conclusion and future recommendation for future works.

CHAPTER 2

LITERATURE REVIEW

2.1 An Overview

The main purpose of controlling a gantry crane is transporting the load as fast as possible without causing any excessive swing at the final position. However, most of the common gantry crane results in a swing motion when payload is suddenly stopped after a fast motion [1]. The swing motion can be reduced but will be time consuming. Moreover, the gantry crane need a skillful operator to control manually based on his or her experiences to stop the swing immediately at the right position. The failure of controlling crane also might cause an accident and may harm people and the surroundings.

Various attempts at controlling gantry crane system based on open loop system were proposed. For example, open loop time optimal strategies were applied to the crane by many researchers such as discussed in [2,3]. They came out with poor results because open loop strategy is sensitive to the system parameters (e.g. rope length) and could not compensate for wind disturbances. Another importance of open loop strategy is the input shaping introduced by Karnopp [4], Teo [5] and Singhose [6]. However the input shaping method is still an open-loop approach.

On the other hand, feedback control which is well known to be less sensitive to disturbances and parameter variations [7] is also adopted for controlling the gantry

On the other hand, feedback control which is well known to be less sensitive to disturbances and parameter variations [7] is also adopted for controlling the gantry crane system. Recent work on the gantry crane control system was presented by Omar [1]. The author had proposed PD (proportional + derivative) controllers for both position and anti-swing controls. Furthermore, a fuzzy-based intelligent gantry crane system has been proposed [8]. The proposed fuzzy logic controllers consist of position as well as anti-swing controllers. The fuzzy logic controllers were designed based on the information on the skillful operators and without the need of crane model and its parameters. The performance of the proposed intelligent gantry crane system had been evaluated experimentally on a lab-scale gantry crane. It was shown that the proposed system has a good positioning performance as well as a good capability to suppress the swing angle in comparison with the crane controlled by the PID (proportional + integral + derivative) controllers [8].

However, most of the feedback control system proposed needs sensors for measuring the cart position as well as the load swing angle. In addition, designing the swing angle measurement of the real gantry crane system, in particular, is not an easy task since there is a hoisting mechanism. Some researches have also focused on control schemes with vision system that is more feasible because the vision sensor is not located at the load side. The drawbacks of the vision system, among those are difficult maintenance and high cost [9].

During the operation of crane system in the container yard, it is necessary to control the crane trolley position so that the swing of the hanging container is minimized. Recently, an automatic control system with high speed and rapid transportation is required. Choi et al. have proposed a neural network two degree of freedom PID controller to control the swing motion and trolley position. As the gantry crane has lots of dynamic characteristics, PID parameters must be changed in varying conditions automatically. At these points, it is important to tune the parameters of the PID control adaptively using a neural network self tuner [10].

Pieper and Surgeno at December 1994 have proposed a single input discrete time sliding mode control for a gantry crane problem. The controller is applied to a simulated pneumatically actuated cart positioning system. The cart tracks a set point in position while steadying a suspended pendulum. Actuators are three valued solenoid operators and pulse-width modulation is used between the control law and the valve [11].

Positioning a crane swinging load, at the bottom end of a cable, by moving a gantry trolley at the top, involves resolving the apparently conflicting demands of exact load positioning and active swing damping. Proposed control strategies to date have been open-ended, involving asymptotic approach to final rest positions. By contrast, a new control strategy, assuming an idealised cable, stops the load dead, exactly at the target, in a finite time, for all but the shortest manoeuvres [12].

The proposed method is easier to derive and implement than the time optimal control schemes and does not require the feedback of adaptive controllers. Rather than attempt to obtain exactly zero residual vibration, which is a practical impossibility, the technique yields non-zero, but low levels of vibration. The control technique investigated here is input shaping – a feed-forward technique that generates a command signal that is self-canceling. Input shaping is implemented in real time by convolving the command signal with an impulse sequence. The process has the effect of placing zeros at the locations of the flexible poles of the original system. An early form of input shaping was posicast control proposed in the late 1950's [13]. More recently, a form of posicast control was successfully applied to the transport of suspended objects [14]. Posicast control is based on a simple linear model and is, unfortunately, very sensitive to modeling errors [15, 16]. When a crane hoists its payload, the system frequency changes, and therefore, posicast control will result in some amount of residual vibration.

Robust input shaping techniques has recently been proposed [15, 17] and shown to work effectively on long-reach manipulators [18], as well as on configuration-dependent systems [19]. An IIR filtering technique related to input shaping has been proposed for controlling suspended payloads [20]. Input shaping has been shown to be effective for controlling oscillation of gantry cranes when the load does not undergo hoisting [21, 22]. Experimental results also indicate that shaped commands can be of benefit when the load is hoisted during the motion [23].

The effectiveness of gantry cranes is often limited by both the transient sway and the residual oscillation of the payload. If the crane acts large like a pendulum, then experienced crane operators can eliminate much of the residual sway by causing a deceleration oscillation that cancels the oscillation induced during acceleration. The success of this approach depends largely on the skill and diligence of the operator.

The feed-forward control technique of input shaping can be used to reduce the crane sway. Input shaping is easier to derive and implement than time-optimal control schemes and does not require the feedback mechanisms of closed loop and adaptive controllers. Input shaping is implemented in real time by convolving the command signal with an impulse sequence (an input shaper). This process is illustrated in Figure 1 with a pulse input and an input shaper containing three positive impulses. Note that the shaped input that results from the convolution has a rise time that is longer than the unshaped input by an amount equal to the duration of the input shaper.

Input shaping is a form of Finite Impulse Response (FIR) filtering that places zeros near the locations of the original system's flexible poles. The impulse amplitudes are equivalent to the filter coefficients. The impulse amplitudes and time locations are determined by satisfying a set of constraint equations. Input shaping has been shown to be effective for controlling oscillation of single pendulum gantry cranes [21, 22].

The industrial use of gantry cranes in ship yards is ever increasing, with a demand for greater safety and faster transfer of loads. The uncontrolled pendulum motion of loads suspended from a gantry crane endangers both the operating personnel and the often fragile load being transported. The crane operator, by the skillful manual drive of the gantry controls, ensures that this unavoidable pendulum motion subsides as quickly as possible. Since extended loading and unloading time is costly. Increasingly however, relatively high speed operating conditions mean that manual suppression of load swing by the operator is not possible, so alternatively mechanical or control engineering solutions have to be found. Mechanical solutions such as cable bracing or scissor-action systems are extremely expensive to install and maintain. Active crane swing compensation, on the other hand is a relatively inexpensive means of achieving greater safety and faster transfer of loads. There has recently been significant research addressing the problem of modeling and controlling gantry cranes. Butler [24] develops a dynamic mathematical model for an overhead gantry crane, but he and Forest [25] assume that the cable sway angle is very small in order to linearize the nonlinear system. A controller was then designed for this linear system. Unfortunately, when the acceleration of the load is not small with respect to gravitational acceleration, the assumptions made will not be justified. Kenison [26] has gone on to develop a model for complex loads that do not approximate simple pendulum motion. However, the control algorithm he uses is input shaping, where he uses a feed-forward system that is susceptible to output disturbances such as wind forces on the container, which are of particular concern in windy coastal regions such as the Eastern Cape in South Africa.

CHAPTER 3

METHODOLOGY

3.1 Introduction

This section described the methods used to reduce sway angle by using hybrid input shaping and PID control schemes. The methods explained by this action are very important procedures in order to ensure the flow of research move smoothly as planned. The methodology of this research is divided into three major sections such as:-

- i. Modeling of gantry crane
- ii. Design and develop hybrid input shaping and PID control schemes
- iii. Simulation and experiment of gantry crane system

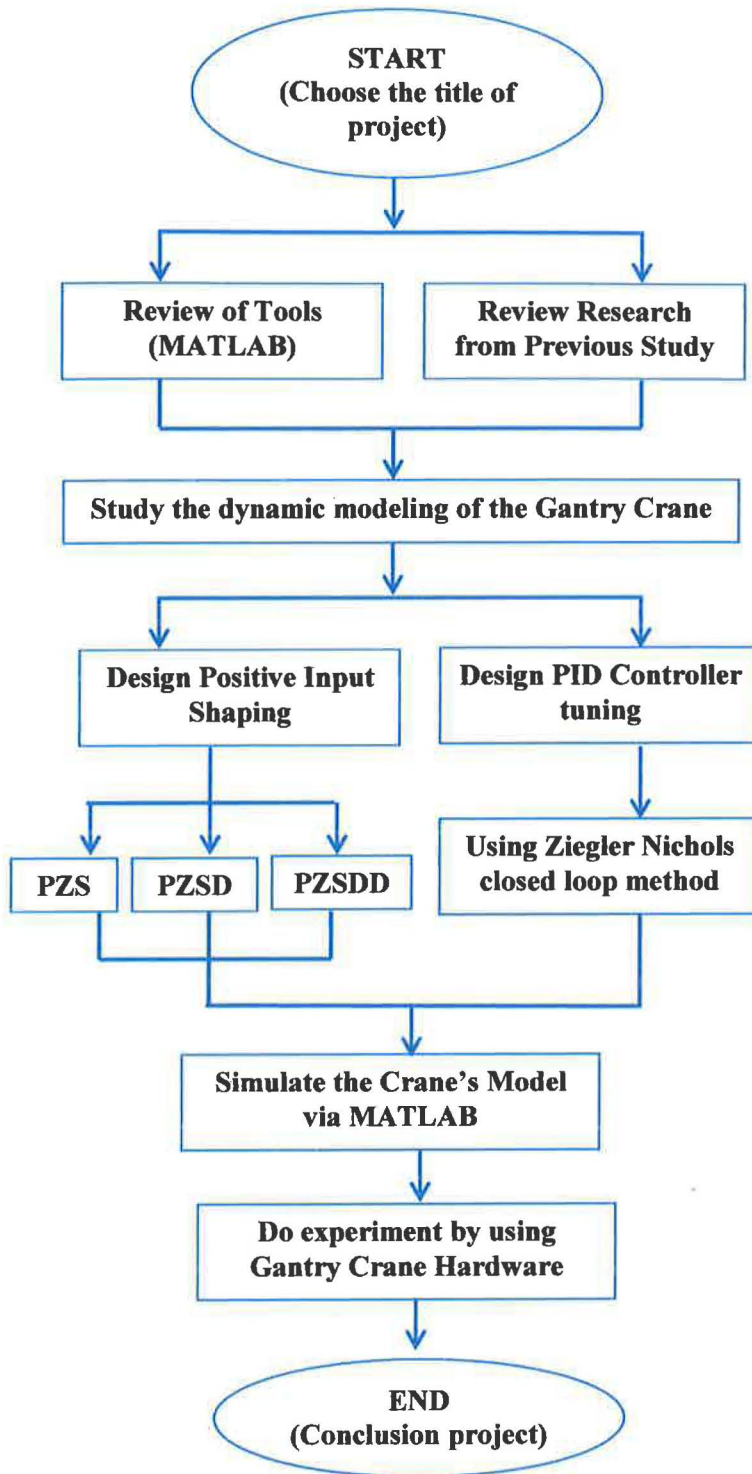


Figure 3.1: Work Methodology

3.2 Modeling of gantry crane

Modeling of a gantry crane is needed to represent the system that's been focused in order to do an analysis and further work. This involves obtaining the dynamic characteristic of the system. With dynamic analysis, it can predict such a problem, before a system is built.

The two-dimensional gantry crane system with its payload considered in this work is shown in Figure 3.2, where x is the horizontal position of the cart, L is the length of the rope, θ is the sway angle of the rope, M and m is the mass of the cart and payload respectively. In this simulation, the cart and the payload can be considered as point masses and are assumed to move in two-dimensional, x - y plane. The tension force that may cause the hoisting rope is also ignored. In this study the length of the cart, $L = 0.5$ m, $M = 2.49$ kg, $m = 0.5$ kg and $g = 9.81$ m/s² is considered.

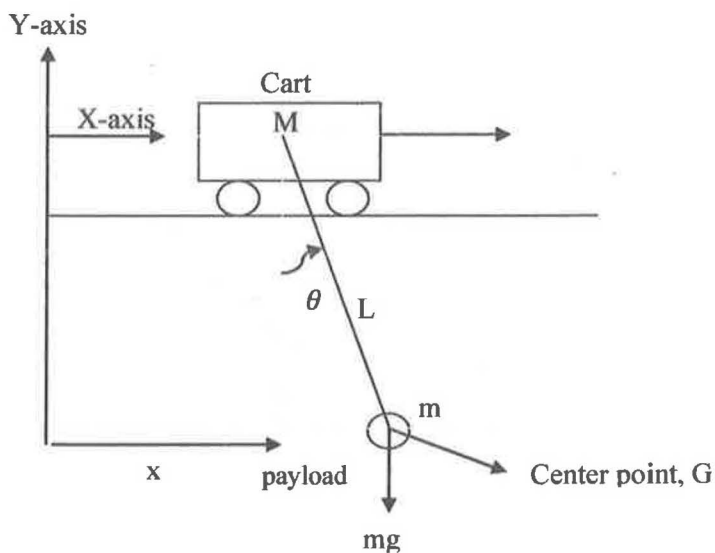


Figure 3.2: Gantry Crane Model

3.2.1 Specifications of the lab-scale gantry crane

The detail specification of the lab-scale gantry crane system is shown in Table 3.1. The straight line motion of the ball screw moves the cart that is connected to it and the pendulum angle that is connected to the cart is controlled. The gantry crane system requires two sensors and the pendulum angle is recognized by the encoder that is connected to the pendulum. The location of the cart is recognized by the encoder that is connected to the motor as shown in Figure 3.3.

Table 3.1: Lab-scale gantry crane specifications

	Item	Specification
Mechanical	W x L x H (mm)	1330 x 200 x 250
	Length of pendulum (L)	0.5 m
	Weight of pendulum (M)	0.5 Kg
	Weight of the cart (m)	2.49 Kg
	Displacement movement	900 mm
	Ball screw pitch	12.7 mm
Electrical	Motor output	24 V, 60 W
	Maximum rotation of motor	3800 rpm
	Encoder Pulse	4000 pulse
	Motor input voltage	0 – 5 V



Figure 3.3: Gantry Crane Pendulum Hardware

3.2.2 Dynamic modeling of gantry crane

This section provides a brief description of the modeling of the gantry crane system. The Euler-Lagrange formulation is considered in characterizing the dynamic behavior of the crane system incorporating payload. The kinetic and potential energy of the whole system is given by:

$$T = \frac{1}{2} M \dot{x}^2 + \frac{1}{2} m (\dot{x}^2 + \dot{l}^2 + l^2 \dot{\theta}^2 + 2x\dot{l}\sin\theta + 2x\dot{l}\theta\cos\theta)$$

The potential energy can be formulated by:

$$U = -mgl \cos\theta \quad (3.2)$$

Using Lagrange equation:

$$\frac{d}{dt} \left(\frac{dL}{dq_j} \right) - \frac{dL}{dq_j} = F_j \quad (3.3)$$

$$u = (m_L + m_c)\ddot{x}_1 + m_L l (\theta \cos\theta \ddot{\theta} - \dot{\theta}^2 \sin\theta) \quad (3.4)$$

$$m_L \ddot{x}_1 \cos\theta + m_L l \ddot{\theta} = -m_L g \sin\theta \quad (3.5)$$

$$\ddot{x}_1 \cos\theta + l \ddot{\theta} = -g \sin\theta$$

From equation (3.4) and (3.5), the equation can be rewritten in the state space equation form:

$$\begin{bmatrix} m_L + m_c & m_L l \cos\theta \\ m_L \cos\theta & m_L l \end{bmatrix} \begin{bmatrix} \ddot{x}_1 \\ \ddot{\theta} \end{bmatrix} = \begin{bmatrix} m_L \dot{\theta}^2 \sin\theta + u \\ -m_L g \sin\theta \end{bmatrix} \quad (3.7)$$

$$\begin{bmatrix} \ddot{x}_1 \\ \ddot{\theta} \end{bmatrix} = \begin{bmatrix} \frac{u + m_L \sin \theta (l\dot{\theta}^2 + g \cos \theta)}{m_c + m_L \sin^2 \theta} \\ - \frac{u \cos \theta + m_L \sin \theta (g + l\dot{\theta}^2 \cos \theta) + g m_c \sin \theta}{l (m_c + m_L \sin^2 \theta)} \end{bmatrix} \quad (3.8)$$

From the above equation 3.8 is in nonlinear function, it can't be used easily for the purpose of analysis, design and other. In order to get a linear model, linearization must be implemented in the above model. The following condition will satisfy the aim:

$$\cos \theta \approx 1; \sin \theta \approx \theta; \sin^2 \theta \approx 0; \dot{\theta}^2 \approx 0$$

$$x = \begin{bmatrix} \dot{x}_1 \\ \dot{x}_2 \\ \dot{x}_3 \\ \dot{x}_4 \end{bmatrix} = \begin{bmatrix} \dot{x}_1 \\ \dot{x}_2 \\ \dot{\theta} \\ \dot{\theta} \end{bmatrix} = \begin{bmatrix} \text{cart position} \\ \text{cart velocity} \\ \text{bar's angle} \\ \text{bar's angle rate} \end{bmatrix} \quad (3.9)$$

The linear model of the uncontrolled system can be represented in a state-space form as shown in equation by assuming the change of rope and sway angle are very small.

3.2.3 State space representation of the system

The state space of gantry crane is represents in equation 3.10 as show below

$$\begin{aligned} x &= Ax + Bu \\ y &= Cx + Dx \end{aligned} \quad (3.10)$$

$$\dot{x} = \begin{bmatrix} \dot{x}_1 \\ \dot{x}_2 \\ \dot{x}_3 \\ \dot{x}_4 \end{bmatrix} = \begin{bmatrix} \dot{x}_1 \\ \dot{x}_2 \\ \dot{\theta} \\ \dot{\theta} \end{bmatrix} = \begin{bmatrix} 0 & 0 & 1 & 0 \\ 0 & 0 & 0 & 1 \\ 0 & \frac{m \cdot g}{M} & 0 & 0 \\ 0 & \frac{-((M+m) \cdot g)}{M \cdot L} & 0 & 0 \end{bmatrix} = \begin{bmatrix} \dot{x}_1 \\ \dot{x}_2 \\ \dot{\theta} \\ \dot{\theta} \end{bmatrix} + \begin{bmatrix} \dot{0} \\ 0 \\ \frac{1}{M} \\ \frac{-1}{M \cdot L} \end{bmatrix}$$

$$C = [1 \quad 0 \quad 0 \quad 0]$$

$$D = [0]$$

(3.11)

3.2.4 Parameter used in this dynamical equation is as follows:

θ : angle of load swing (rad)

M : mass of the load (kg)

m : mass of the trolley (kg)

L : length of rope (m)

g : gravity acceleration (m/s²)

\ddot{x} : acceleration of trolley (m/s²)

$\ddot{\theta}$: angular acceleration of the load swing (rad/s²)

3.3 Research on positive input shaping techniques

3.3.1 Objective Input Shaping

- i. To determine the amplitude and time location of the impulses based on the natural frequency and damping ratios of the system
- ii. To work as a feed-forward controller which is for controlling the sway angle of the pendulum for reducing vibrations of gantry crane.
- iii. To design and develop command signal that cancels its own vibration based on positive zero sway (PZS), positive zero sway derivative (PZSD) and positive zero sway derivative-derivative (PZSDD) shapers.

3.3.2 Operation of Input Shaping

Positive input shaping was generated through the convolution of the impulse function with bang-bang input. Each of the positive input shaping contains a different value of impulse. An unshaped bang-bang force is used to determine the characteristic parameters of the system for design and evaluation of input shaping control techniques. Figure 3.4 and 3.5 show the illustration and block diagram of input shaping technique.

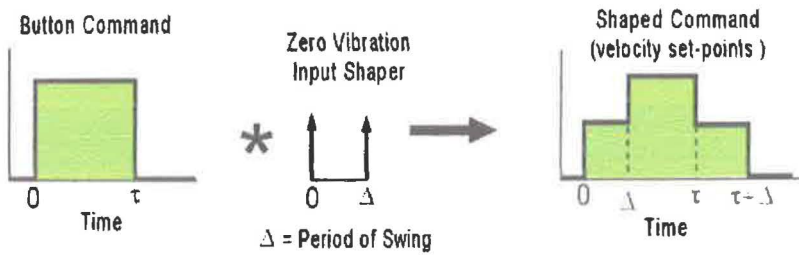


Figure 3.4: Illustration of input shaping technique

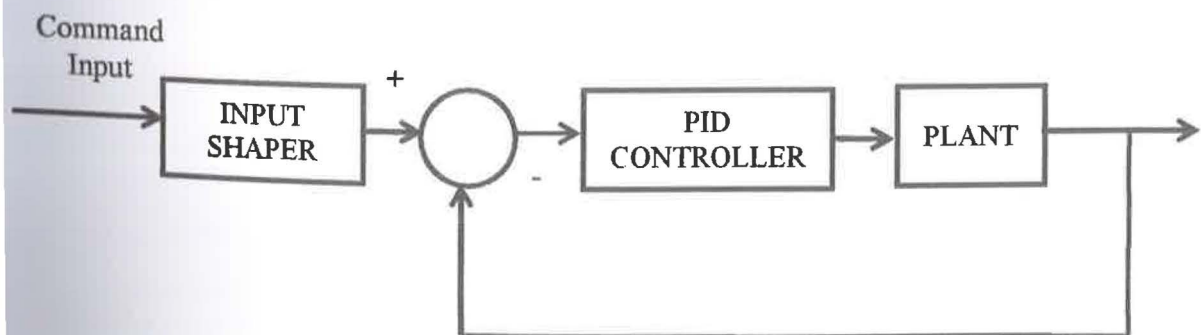


Figure 3.5: Block diagram of input shaping outside closed loop system

3.3.2 Operation of Input Shaping

Positive input shaping was generated through the convolution of the impulse function with bang-bang input. Each of the positive input shaping contains a different value of impulse. An unshaped bang-bang force is used to determine the characteristic parameters of the system for design and evaluation of input shaping control techniques. Figure 3.4 and 3.5 show the illustration and block diagram of input shaping technique.

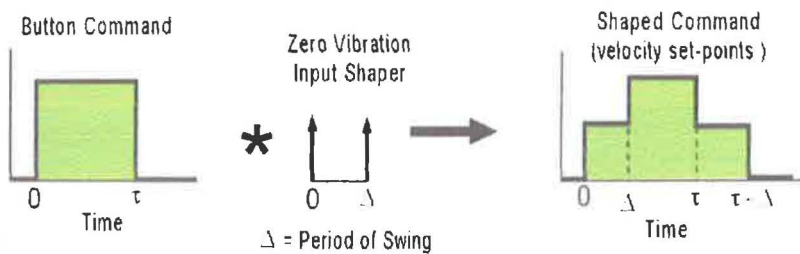


Figure 3.4: Illustration of input shaping technique

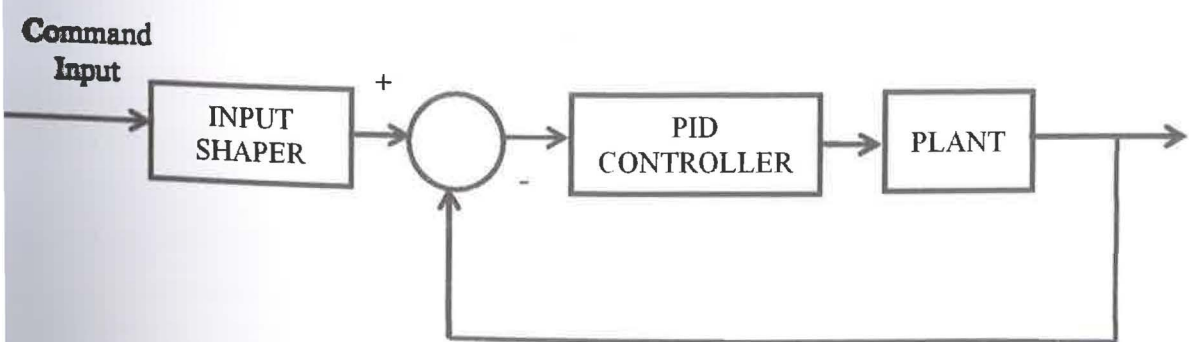


Figure 3.5: Block diagram of input shaping outside closed loop system

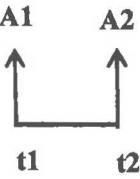
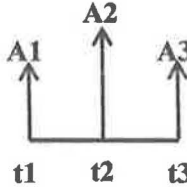
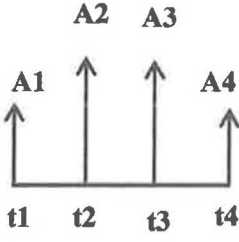
3.3.3 Bang-bang Input Techniques

The bang - bang input of positive input shaping was implemented in real time by convolving the command signal with an impulse sequence. Each of the positive input shaping contains a different value of impulse. This process is illustrated based on positive zero sway (PZS), positive zero sway derivative (PZSD) and positive zero sway derivative-derivative (PZSDD) shapers.

3.3.4 Development of positive input shaping

For this project, positive input shaping controller of anti sway is developed for the system. Based on the previous research, input shaping can reduce the sway of the system significantly. The positive input shaping control scheme will divide into three types which are positive zero sway (PZS), positive zero sway derivative (PZSD) and positive zero sway derivative-derivative (PZSDD). Each of the positive input shaping contains a different value of impulse. Table 3.2 shows the summarized of positive input shaping techniques.

Table 3.2: Positive Input Shaping Techniques

Positive Zero Sway (PZS)	Positive Zero Sway Derivative (PZSD)	Positive Zero Sway Derivative- Derivative (PZSDD)
<ul style="list-style-type: none"> • Contain 2 impulse responses include: <ol style="list-style-type: none"> i. Unity amplitude summation ii. Time optimality constraints <div style="text-align: center; margin-top: 20px;">  </div>	<ul style="list-style-type: none"> • Contain 3 impulse responses include: <ol style="list-style-type: none"> i. Unity amplitude summation ii. Time optimality constraints iii. First order robustness constraint equation. <div style="text-align: center; margin-top: 20px;">  </div>	<ul style="list-style-type: none"> • Contain 3 impulse responses include: <ol style="list-style-type: none"> i. Unity amplitude summation ii. Time optimality constraints iii. Second order robustness constraint equation. <div style="text-align: center; margin-top: 20px;">  </div>

3.3.5 Design equation of Input Shaping Schemes

The design objectives of input shaping are to determine the amplitude and time locations of the impulses in order to reduce the detrimental effects of system flexibility. These parameters are obtained from the natural frequencies and damping ratios of the system. The corresponding design relations for achieving a zero residual single-mode sway of a system and to ensure that the shaped command input produces the same rigid body motion as the unshaped command yields a two-impulse sequence namely zero-sway (ZS) with parameter as shown in equation (3.12)

$$\begin{aligned}
 t_1 &= 0, & t_2 &= \frac{\pi}{\omega_d} \\
 A_1 &= \frac{1}{1+K}, & A_2 &= \frac{K}{1+K}
 \end{aligned} \tag{3.12}$$

where

$$K = e^{\frac{-\xi \pi}{\sqrt{1-\xi^2}}}$$

$$\omega_d = \omega_n \sqrt{1 - \xi^2}$$

$$\omega_n = \sqrt{\frac{g}{l} \left(\frac{M+m}{M} \right)}$$

(ω_n and ξ representing the natural frequency and damping ratio respectively) and t_j and A_j are the time location and amplitude of impulse j respectively. This yields a three-impulse and four-impulse sequence namely zero-sway-derivative (ZSD) and zero sway- derivative (ZSDD) with parameter as shown in equations (3.13) and (3.14) respectively:

$$t_1 = 0, \quad t_2 = \frac{\pi}{\omega_d}, \quad t_3 = \frac{2\pi}{\omega_d} \tag{3.13}$$

$$A_1 = \frac{1}{1+2K+K^2}, \quad A_2 = \frac{2K}{1+2K+K^2}, \quad A_3 = \frac{K^2}{1+2K+K^2}$$

$$t_1 = 0, \quad t_2 = \frac{\pi}{\omega_d}, \quad t_3 = \frac{2\pi}{\omega_d}, \quad t_4 = \frac{3\pi}{\omega_d} \tag{3.14}$$

$$A_1 = \frac{1}{1+3K+3K^2+K^3}, \quad A_2 = \frac{3K}{1+3K+3K^2+K^3},$$

$$A_3 = \frac{3K^2}{1+3K+3K^2+K^3}, \quad A_4 = \frac{K^3}{1+3K+3K^2+K^3}$$

3.3.6 Advantages of Input Shaping

- i. Designing an input shape does not require an analytical model of the system; it can be generated from simple, empirical measurements of the actual physical system.
- ii. Input shaping does not affect the stability of the closed loop system in any way. It simply modifies the command signal to the system so that all moves, regardless of length, are vibration free.
- iii. Input shaping does not require a dedicated transducer to measure the vibrations. It can be applied successfully to systems where vibrations cannot be observed at the feedback transducers.

3.4 Research on PID controller techniques

Proportional-Integrated Derivative (PID) control is the most popular feedback controller used within the process industries involved in controlling the crane position. PID also provides a constant system output at a specified set point.

3.4.1 Objectives PID control

- i. To determine the proportional, integral and derivative scaling coefficients in the control equation.
- ii. To work as a feedback controller which is for controlling the position of crane for reducing vibrations of gantry crane.
- iii. To effectively tune a PID controller algorithm

3.4.2 Combinational of all three modes (P, I and D)

i. In Time Domain

$$MV(t) = K_p \left(e(t) + \frac{1}{T_i} \int_0^t e(t) dt + T_d \frac{de(t)}{dt} + I \right)$$

ii. In Frequency Domain

$$MV(s) = K_p \left(1 + \frac{1}{T_i s} + T_d s \right) E(s)$$

Where,

MV : Manipulated Variable

K_p : Proportional gain

T_i : Integral time

T_d : Derivative time

$e(t)$: error signal

The desired closed loop dynamics is obtained by adjusting the three parameters such as Proportional gain (K_p), Integral time (T_i) and Derivative time (T_d), often iteratively by "tuning" and without specific knowledge of a plant model. Stability can often be ensured using only the proportional term. The integral term permits the rejection of a step disturbance. The derivative term is used to provide damping or shaping of the response.

3.4.3 PID control procedures in closed loop system:

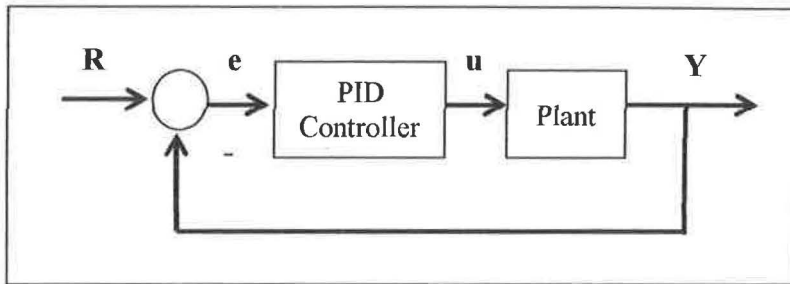


Figure 3.6: Block Diagram of a PID Control

Figure 3.6 shows the block diagram of a PID controller in a closed loop system. The variable (e) represents the tracking error, the difference between the desired input value (R) and the actual output (Y).

This error signal (e) will be sent to the PID controller, and the controller computes both the derivative and the integral of this error signal. The signal (u) just past the controller is now equal to the K_p times the magnitude of the error plus the K_i times the integral of the error plus the K_d times the derivative of the error. This signal (u) will be sent to the plant, and the new output (Y) will be obtained. This new output (Y) will be sent back to the sensor again to find the new error signal (e). The controller takes this new error signal and computes its derivative and its integral again. This process goes on and on.

The PID controller calculate the control signal $u(t)$ as mathematically processing the error signal as shown in formula (3.15)

$$u(t) = K_p e(t) + K_i \int e(t) dt + K_d \frac{de(t)}{dt} \quad (3.15)$$

The improvement of the PID controller performance depends on the method that gains are defined. When (3.15) is converted into Laplace transform, the result is shown in the formula (3.16)

$$U(s) = \left(K_p s + K_i \frac{1}{s} + K_d s \right) E(s) \quad (3.16)$$

$$\frac{U(s)}{E(s)} = \frac{K_p s^2 + K_i s + K_d}{s}$$

The PID control scheme is named after its three correcting terms, whose sum constitutes the manipulated variable (MV) as shown in Figure 3.7

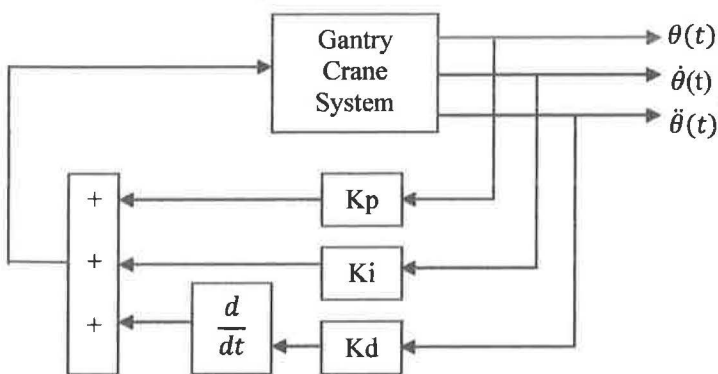


Figure 3.7: The PID controller structure

3.4.4 Characteristics of PID

A proportional controller (K_p) reduces the rise time of the plant response, but it cannot eliminate the steady-state error. An integral control (K_i) can remove the steady-state error, but worsen the characteristics of the transient response. However the differential gain K_p can improve the stability of the system, so it can reduce the overshoot and improve the characteristic of the transient response. A derivative control (K_d) can increase the stability of the system, reduce the overshoot, and improve the transient response. The effects of each of controllers K_p , K_d , and K_i on a closed-loop system are summarized in the Table 3.3. The change coefficients of any one can change other two coefficients.

Table 3.3: The characteristics of P, I, D controllers

CL RESPONSE	RISE TIME	OVERSHOOT	SETTLING TIME	S-S ERROR
K_p	Decrease	Increase	Small Change	Decrease
K_i	Decrease	Increase	Increase	Eliminate
K_d	Small Change	Decrease	Decrease	Small Change

The detail of each characteristic of the response for proportional gain (K_p), integral gain (K_i) and derivative gain (K_d) are explained as below (i-iii)

i. Proportional Gain

The proportional term makes a change to the output that is proportional to the current error value. The proportional response can be adjusted by multiplying the error by a constant proportional gain (K_p). The proportional term is given by:

$$P_{out} = K_p e(t)$$

where, P_{out} is an output of proportional, K_p is a tuning parameter of proportional gain, e is an error and t is a time.

When the value of K_i and K_d held constant, a high proportional gain results in a large change in the output for a given change in the error. If the proportional gain is too high, the system can become unstable. In contrast, a small gain results in a smaller output response to a large input error, and a less responsive or less sensitive controller. While if the proportional gain is too low, the control action may be too small when responding to system disturbances as shown in Figure 3.8.

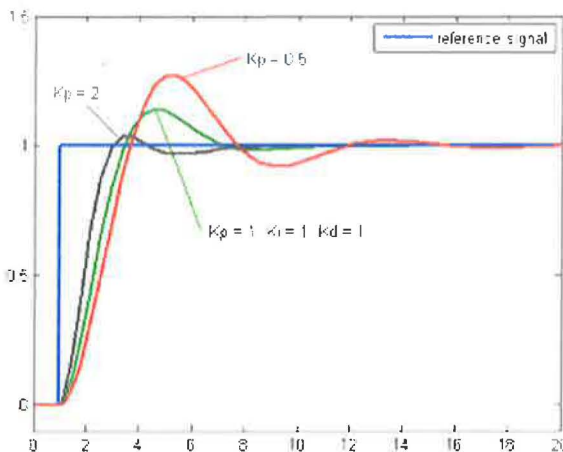


Figure 3.8: Plot of PV vs time, for three values of K_p

ii. Integral Gain

The contribution of the integral term is proportional to both the magnitude of the error and the duration of the error. The integral in a PID controller is the sum of the instantaneous error over time and gives the accumulated offset that should have been corrected previously. The accumulated error is then multiplied by the integral gain (K_i) and added to the controller output. The integral term is given by:

$$I_{out} = K_i \int_0^t e(\tau) d\tau$$

where, I_{out} is an output of integral, K_i is a tuning parameter of integral gain, e is an error, τ is a dummy integration variable and t is a time.

When the value of K_p and K_d held constant, the integral term accelerates the movement of the process towards set-point and eliminates the residual steady-state error that occurs with a pure proportional controller. However, since the integral term responds to accumulated errors from the past, it can cause the present value to overshoot the set-point value. The comparison of those different values of K_i as shown in Figure 3.9.

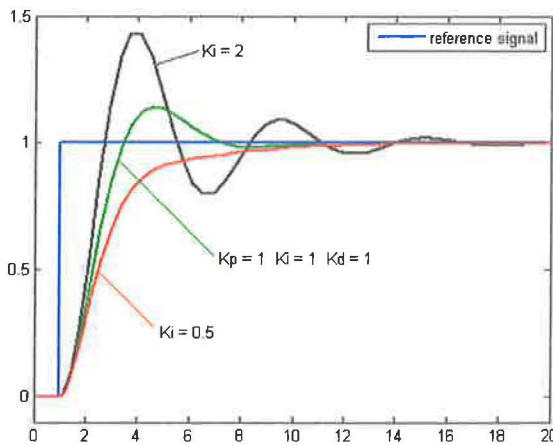


Figure 3.9: Plot of PV vs time, for three values of K_i

iii. Derivative Term

The derivative of the process error is calculated by determining the slope of the error over time and multiplying this rate of change by the derivative gain K_d . The magnitude of the contribution of the derivative term to the overall control action is termed the derivative gain, K_d . The derivative term is given by:

$$D_{out} = K_d \frac{d}{dt} e(t)$$

where, D_{out} is an output of derivative, K_d is a tuning parameter of derivative gain, e is an error and t is a time.

When the value of K_p and K_i held constant, the derivative term slows the rate of change of the controller output. Derivative control is used to reduce the magnitude of the overshoot produced by the integral component and improve the combined controller-process stability. However, differentiation of a signal amplifies noise and thus this term in the controller is highly sensitive to noise in the error term, and can cause a process to become unstable if the noise and the derivative gain are sufficiently large. The comparison of those different values of K_d is shown in Figure 3.10

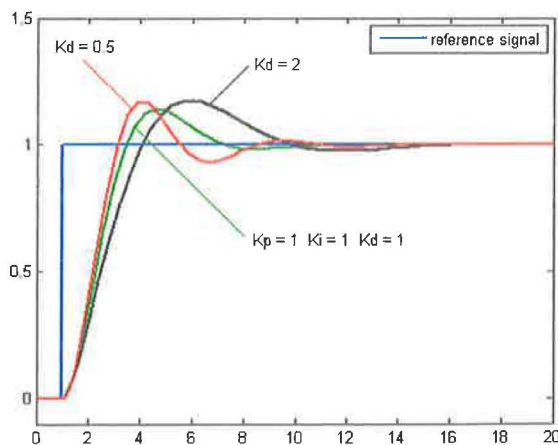


Figure 3.10: Plot of PV vs time, for three values of K_d

3.4.5 Ziegler–Nichols Frequency Response Method (second method)

The second method targets plants that can be rendered unstable under proportional control. The technique is designed to result in a closed loop system with 25% overshoot. Ziegler and Nichols proposed rules for determining the values of the proportional gain (K_p), integral time (T_i), and the derivative time (T_d) based on transient response characteristics of a given plant.

For the Ziegler-Nichols Frequency Response Method, the critical gain, K_{cr} and the critical period, P_{cr} have to be determined first by setting the $T_i = \infty$ and $T_d = 0$. Increase the value of K_p from 0 to a critical value, adjust gain to make the oscillations continue with a constant amplitude as shown in Figure 3.11, the value of K_{cr} is at which the output first exhibits sustained oscillation. Table 3.4 shows the formula of controller tuning parameters for the second method of Ziegler-Nichols.

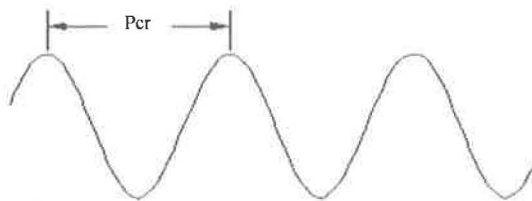


Figure 3.11: Step Response for Critical Period (1 cycle)

Table 3.4: Critical Gain (K_{cr}) and Critical Period (P_{cr})

PID TYPE	K_p	T_i	T_d
P	$0.5 K_{cr}$	∞	0
PI	$0.45 K_{cr}$	$\frac{P_{cr}}{1.2}$	0
PID	$0.6 K_{cr}$	$1/\left(\frac{P_{cr}}{2}\right)$	$\frac{P_{cr}}{8}$

$$K_{cr} = \frac{1}{|G_p(j\omega_c)G_v(j\omega_c)G_s(j\omega_c)|}$$

$$P_{cr} = \frac{2\pi}{(\omega_c)}$$

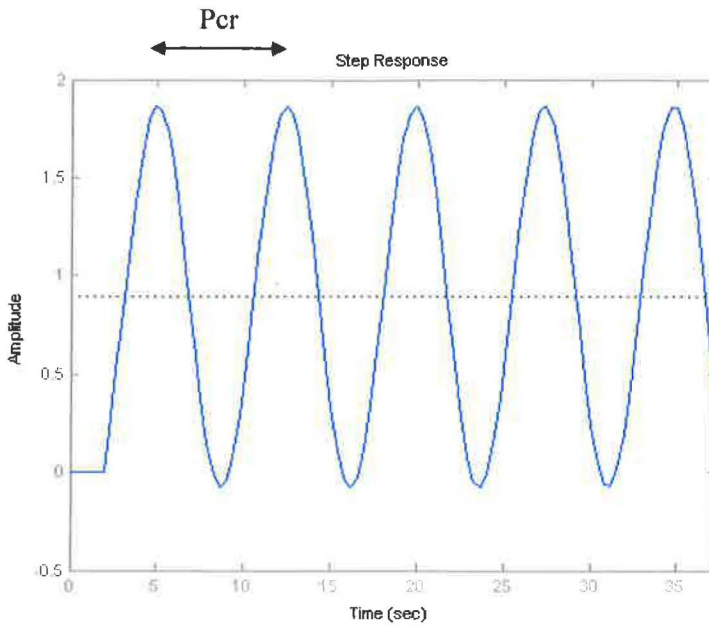


Figure 3.12: Sustained oscillation response

From the graph in Figure 3.12, tuning of PID Mode has been determined as shown in Table 3.5:-

Table 3.5: Calculation of PID based on Ziegler Nichols (second method)

Value Critical gain and period	K_p	T_i	T_d
$K_{cr} = 1$ $P_{cr} = 5$	$= 0.6 * K_{cr}$ $= 0.6 * 1$ $= 0.6$	$= 1 / \left(\frac{P_{cr}}{2} \right)$ $= 1 / \left(\frac{5}{2} \right)$ $= \frac{1}{2.5}$ $= 0.4$	$= \frac{P_{cr}}{8}$ $= \frac{5}{8}$ $= 0.625$
Tuning PID	$K_p = 0.6$	$T_i = 0.4$	$T_d = 0.625$

3.5 Simulation Studies

Figure 3.13 shows a block diagram of sway control using hybrid input shaping and PID controller schemes for the gantry crane system. The systems are then built in the MATLAB software. The output signal that generated from simulation will give preliminary results for hybrid input shaping and PID control schemes. The result will be used as reference for experimental of reducing sway angle of the gantry crane system. Simulation result of the response is presented in time and frequency domains.

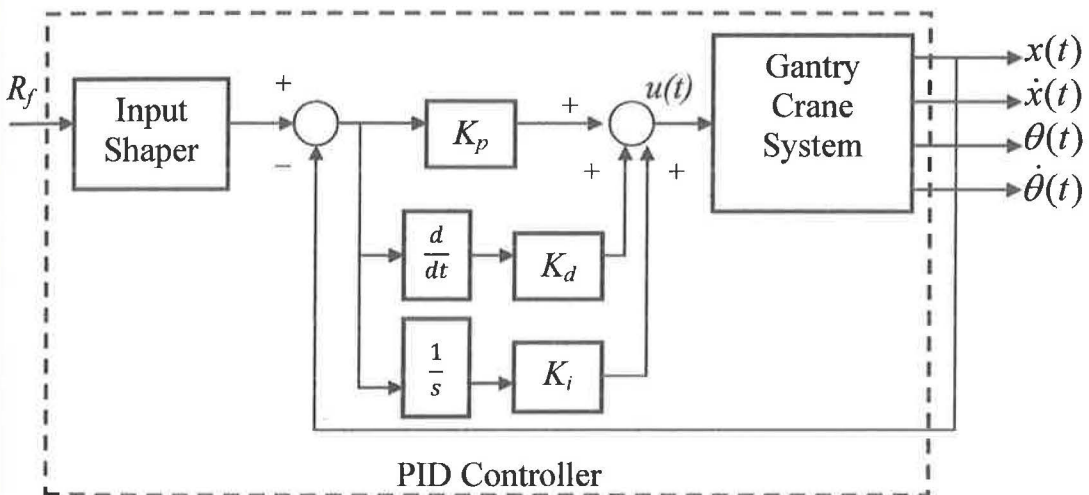


Figure 3.13: Block diagram for hybrid input shaping and PID control schemes

In the simulation process, two controllers have been used to control the sway of gantry crane. Input shaping has been used as a feed-forward controller and PID have been used as a feedback controller. The output of the system is represented in term of sway angle of the pendulum, velocity of the pendulum, the position of the cart and the velocity of the cart. The whole system for the simulation work is shown in Figure 3.14, which is executed by a combination of each block in Figure 3.15

3.5 Simulation Studies

Figure 3.13 shows a block diagram of sway control using hybrid input shaping and PID controller schemes for the gantry crane system. The systems are then built in the MATLAB software. The output signal that generated from simulation will give preliminary results for hybrid input shaping and PID control schemes. The result will be used as reference for experimental of reducing sway angle of the gantry crane system. Simulation result of the response is presented in time and frequency domains.

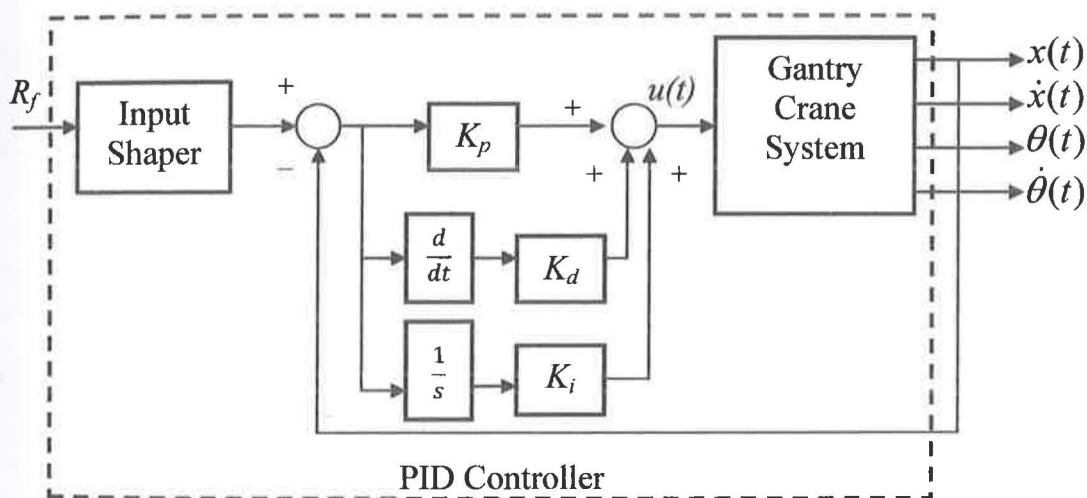


Figure 3.13: Block diagram for hybrid input shaping and PID control schemes

In the simulation process, two controllers have been used to control the sway of gantry crane. Input shaping has been used as a feed-forward controller and PID have been used as a feedback controller. The output of the system is represented in term of sway angle of the pendulum, velocity of the pendulum, the position of the cart and the velocity of the cart. The whole system for the simulation work is shown in Figure 3.14, which is executed by a combination of each block in Figure 3.15

(connection inside the system of input shaping controller) and Figure 3.16 (connection inside the system of PID controller). State space block has been used to implement the 2D modeling of the gantry crane system as shown in Figure 3.17. For the configuration in the system, the parameters can be changed by changing the value of the parameter in m-file as shown in Figure 3.18. For the simulation implementation, the manipulated variables are the initial value of rode position, length of the rode and mass of the rode. The simulation has been executed at the interval of 0.001 second for 10 seconds as shown in Figure 3.19.

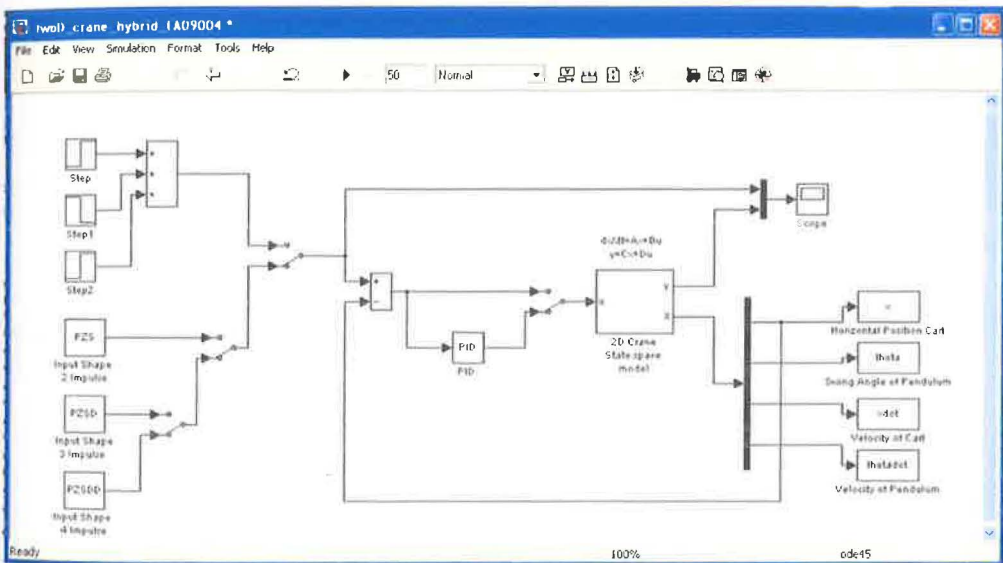


Figure 3.14: Simulink Model of Gantry Crane System

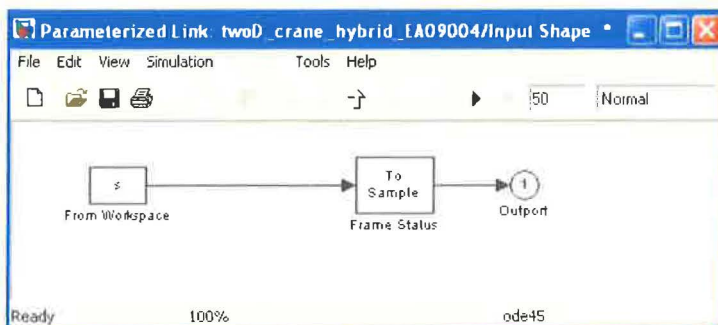


Figure 3.15: Input shaping controller inside the system

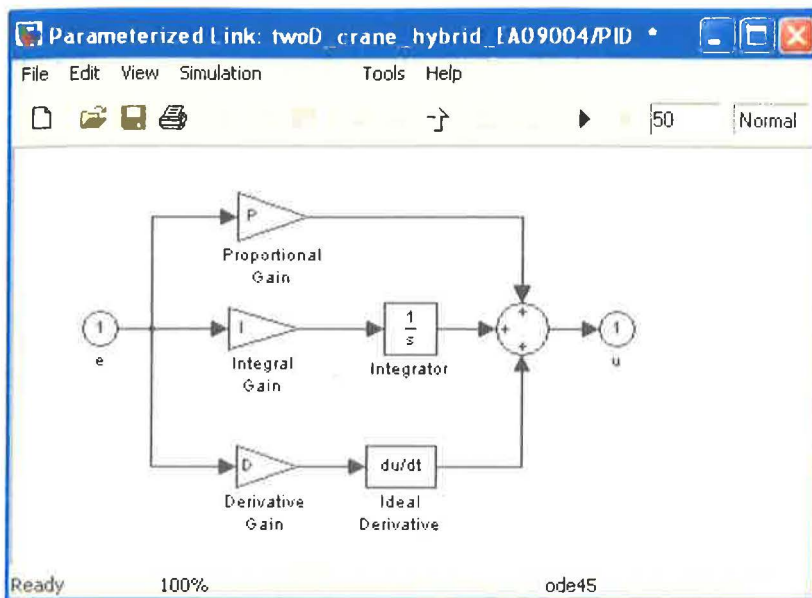


Figure 3.16: PID controller inside the system

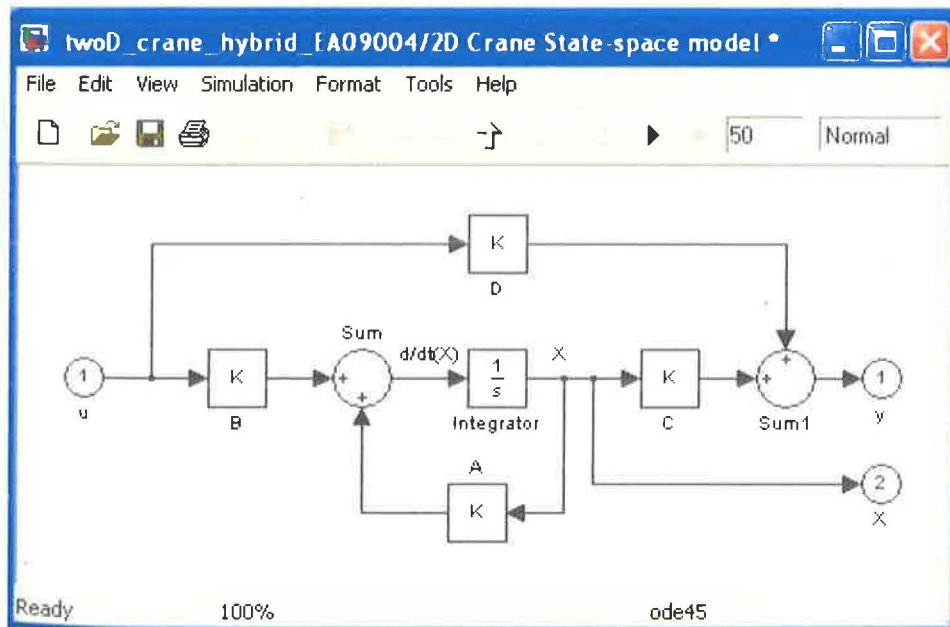
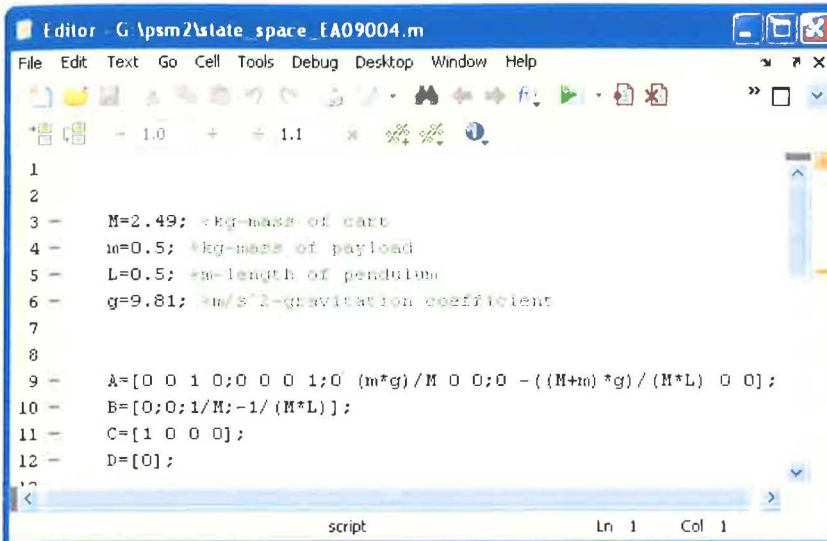


Figure 3.17: 2D modeling of gantry crane inside the system



```

1
2
3 - M=2.49; %kg-mass of cart
4 - m=0.5; %kg-mass of payload
5 - L=0.5; %m-length of pendulum
6 - g=9.81; %m/s^2-gravitation coefficient
7
8
9 - A=[0 0 1 0;0 0 0 1;0 (m*g)/M 0 0;0 -((M+m)*g)/(M*L) 0 0];
10 - B=[0;0;1/M;-1/(M*L)];
11 - C=[1 0 0 0];
12 - D=[0];

```

Figure 3.18: Source code modeling of state space



Figure 3.19: Block Parameter of Input Shaping

3.6 Experimental Studies

The experiments will be conducted by using a gantry crane pendulum system, I/O board hardware, CEM-Tools and MATLAB software, to achieve the same output as the simulation studies. The pendulum system used in this study transmits the rotational power of the motor that is generated as the motor rotates through the ball screw and the rotation is changed into the straight line motion. The straight line motion of the ball screw moves the cart that is connected to it and the pendulum angle that is connected to the cart is controlled. The gantry crane system requires two sensors and the pendulum angle is recognized by the encoder that is connected to the pendulum. The location of the cart is recognized by the encoder that is connected to the motor. The detail specification of the lab-scale gantry crane system is shown in Table 3.1.

The filter algorithm is implemented by using an industrial personal computer (Pentium IV, CPU 2.4GHz). The encoder sensor's signals from the angle and cart motion are connected to the analogue I/O Port of RG-DSPIO01 with a voltage range of -10 V to +10 V. The output of the controller is also sent to the analogue I/O Port of RGDSPIO01 using 25P connector. The hybrid input shaping and PID control techniques algorithm is implemented in CEM-Tool software with the sampling period selected at 1 ms.

3.6.1 Verification of Control Design

The unshaped bang-bang torque input is designed in SIM-Tool to determine characteristic parameters of the system for the design and evaluation of the hybrid input shaping and PID control technique. The suitable values for every step are chosen. The output of the step design must balance between positive and negative

part at Y-axis. The configurations for parameter settings unshaped bang-bang torque input are shown in Figure 3.20-3.22. Figure 3.20 shows the parameter setting in step 1. The bang-bang torque input started at 0.2 sec for X-axis which stated 1 as the initial value and the final value is 2 for the Y-axis. The input signal parameter setting in step 2 is started at 0.5 sec for X-axis while the initial value is 0.0 and the final value is -2 for the Y-axis as shown in Figure 3.21. Then, Figure 3.22 shows the parameter setting in step 3 at 0.8 sec for X-axis whereas for Y-axis, the initial value is 0.0 and the final value is 1.

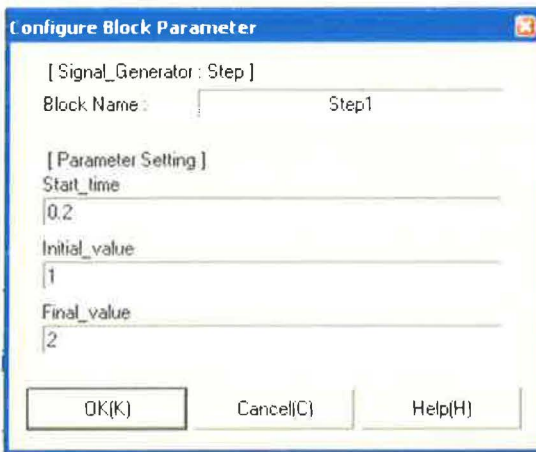


Figure 3.20: Parameter Setting in Step 1

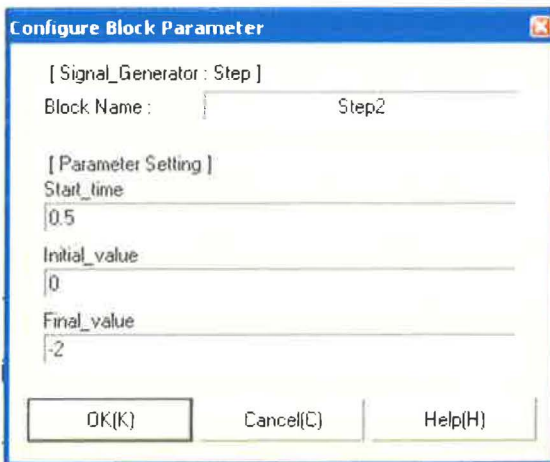


Figure 3.21: Parameter Setting in Step 2

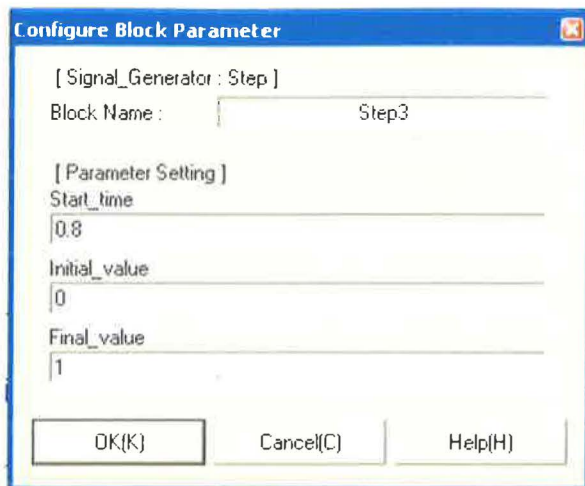


Figure 3.22: Parameter Setting for Step 3

The coding for positive input shaping in M-file mode is converted to CEM mode. The coding is run in CEM mode and the variable is stored in the workspace of SIM-Tools as shown in Figure 3.23-3.24. The variable stored in the workspace is depending on the derivatives of the input shaping. After the coding has been run in CEM-Tools, the results from CEM-Tools then were being transferred to MATLAB to get the final result of sway angle and the horizontal position cart.

The screenshot shows the 'Information Window' with a 'Variables' section expanded. It displays a table of variables with their names, sizes, and types. The variables listed include matrices of various sizes (e.g., 1x2, 1x3, 10x10, 30x30) and scalars. The variable 'PZSDD' is highlighted in blue.

Name	Size	Type
A1a	1 x 2	matrix
A1b	1 x 3	matrix
A1c	1 x 4	matrix
PZS	10...	matrix
PZSD	10...	matrix
PZSDD	10...	matrix
ans	1 x 1	scalar
i	1 x 1	scalar
imp1a	30...	matrix
imp1b	30...	matrix
imp1c	30...	matrix
impa	10...	matrix
impb	10...	matrix
impc	10...	matrix
ip	1 x 1	scalar
k1	1 x 1	scalar
ni	1 x 1	scalar
pi	1 x 1	scalar
sampling...	1 x 1	scalar
shp1a	20...	matrix
shp1b	20...	matrix
shp1c	20...	matrix
simulatio...	1 x 1	scalar
starting...	1 x 1	scalar
t	1 x...	range
tt1a	1 x 2	matrix
tt1b	1 x 3	matrix
tt1c	1 x 4	matrix
u	10...	matrix
v1a	30...	matrix
v1b	30...	matrix
v1c	30...	matrix

Figure 3.23: Variable of Input Shaping in CEM-Tools

The screenshot shows the 'Configure Block Parameter' dialog box. It has a title bar with a close button. The content is organized into sections: '[Signal_Generator : From Workspace]' with a 'Block Name' field containing 'From Workspace'; '[Parameter Setting]' with a 'Matrix_table' field containing 'PZSDD'; and three buttons at the bottom: 'OK(K)', 'Cancel(C)', and 'Help(H)'.

Figure 3.24: Configuration of workspace in CEM-Tools

3.6.2 Data Collection and Analysis Controller Design

The experimental study was developed by using CEM-Tools interface with Gantry Crane Pendulum System Hardware. Figure 3.25-3.28 shows the complete block diagram of SIM-Tools model design with and without controller based on PID control schemes and also interfacing connection between CEM-Tools and Gantry Crane Pendulum System Hardware.

This experiment will collect the data for angle of the sway and position of the cart. Firstly, start the simulation with initial block diagram followed by SIM-Tool model design. The Gantry Crane Pendulum System hardware will react when the block diagram of SIM-Tool start. The cart will swing-up based on the program. Then the data automatically save in variables of CEM-Tool. The data from CEM-Tool will convert into the workspace of MATLAB. The experiment is continuing to find the natural frequency ω_n by taking the highest amplitude in the power spectral density (PSD) response and then multiply it with 2π to get the natural frequency that will be used in CEM-Tools software. Then, the final output graph for angle of the sway and position of the cart are generated from MATLAB source code.

The results of the experiment are compared between a simulation design with and without a controller. Comparisons of the time response specification based on hybrid input shaping and PID controller technique are recorded. The time response specifications of rise time, settling time, overshoot and attenuation sway angle of the pendulum will indicate which of techniques in input shaping is more efficient to reduce a sway angle of the gantry crane system. Finally, a comparative assessment of the control techniques is presented and discussed.

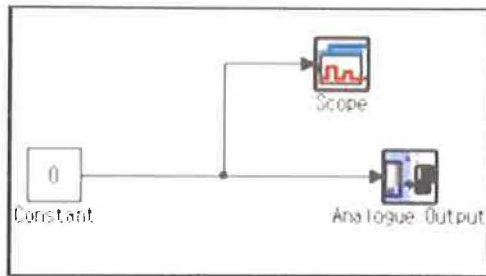


Figure 3.25: SIM-Tool Initial Block Diagram

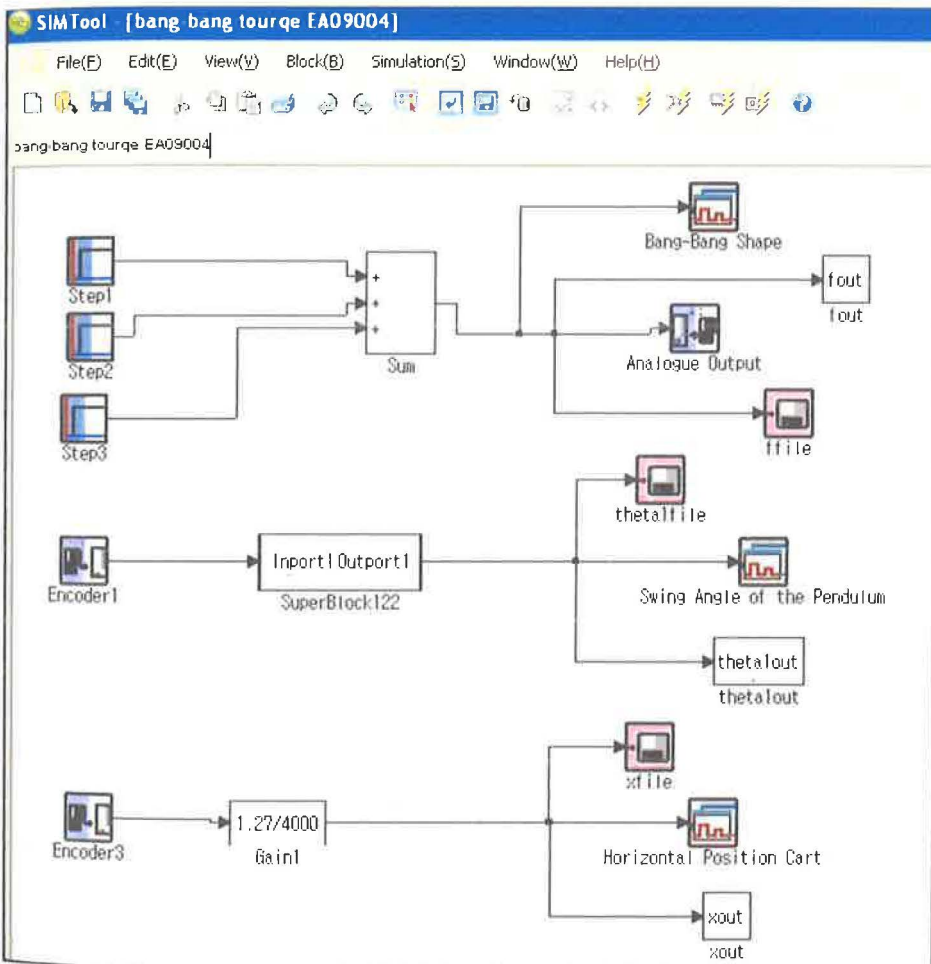


Figure 3.26: Model of gantry crane design without controller

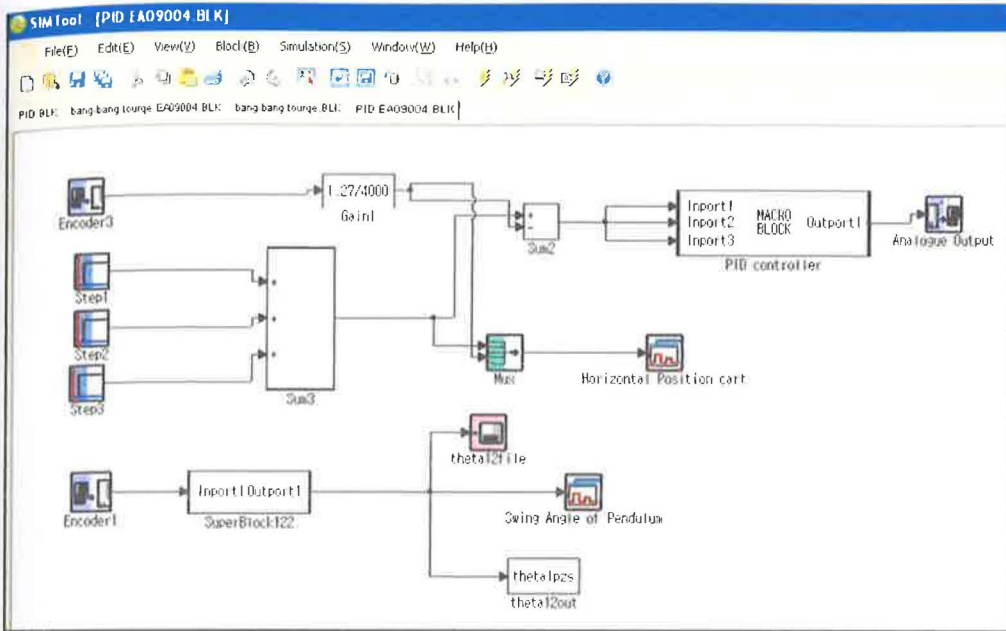


Figure 3.27: Model of gantry crane design with controller



Figure 3.28: Interfacing connection between CEM-Tools and Gantry Crane Pendulum

CHAPTER 4

RESULTS AND DISCUSSIONS

4.1 Introduction

This chapter is discussing about all results which are simulation and experimental results and followed with discussions for this project. The simulation studies were done using MATLAB and experimental studies were done using CEM-Tools with Gantry Crane Pendulum. The results will divide into four major sections:

- i. Simulation results using MATLAB for hybrid input shaping and PID controller
- ii. Experimental results using CEM-Tools with Real Gain swing-Up Inverted Pendulum
- iii. Result analysis
- iv. Comparative Assessment

4.2 Comparative Assessment of Simulation

The bang-bang input voltage of $\pm 1.5\text{V}$ is applied to the cart of the gantry crane system. To study the effectiveness of sway suppression, PZS, PZSD and PZSDD shapers with PID controller are designed based on the sway frequencies and damping ratios of the gantry crane system. The first mode, sway of the system is considered, as these dominate the dynamic of the system. The responses of the gantry crane system to the unshaped input were analyzed in time-domain and frequency domain (spectral density). These results were considered as the system response to the unshaped input and will be used to evaluate the performance of the input shaping schemes.

4.3 Simulation result using MATLAB software

In simulation, result of sway angle, horizontal position cart and power spectra density values were presented by using two controllers which are for feed-forward controller, input shaping has been used to control the sway angle of the pendulum and for feedback controller, PID has been used to control the crane position. Figure 4.1 shows a block diagram of a gantry crane by using hybrid input shaping and PID control techniques, which has been studied to reduce the sway of gantry crane. Performances of the input shaper and PID control are examined in terms of swing angle reduction and time response specifications. Finally a comparative assessment of the control techniques is presented and discussed.

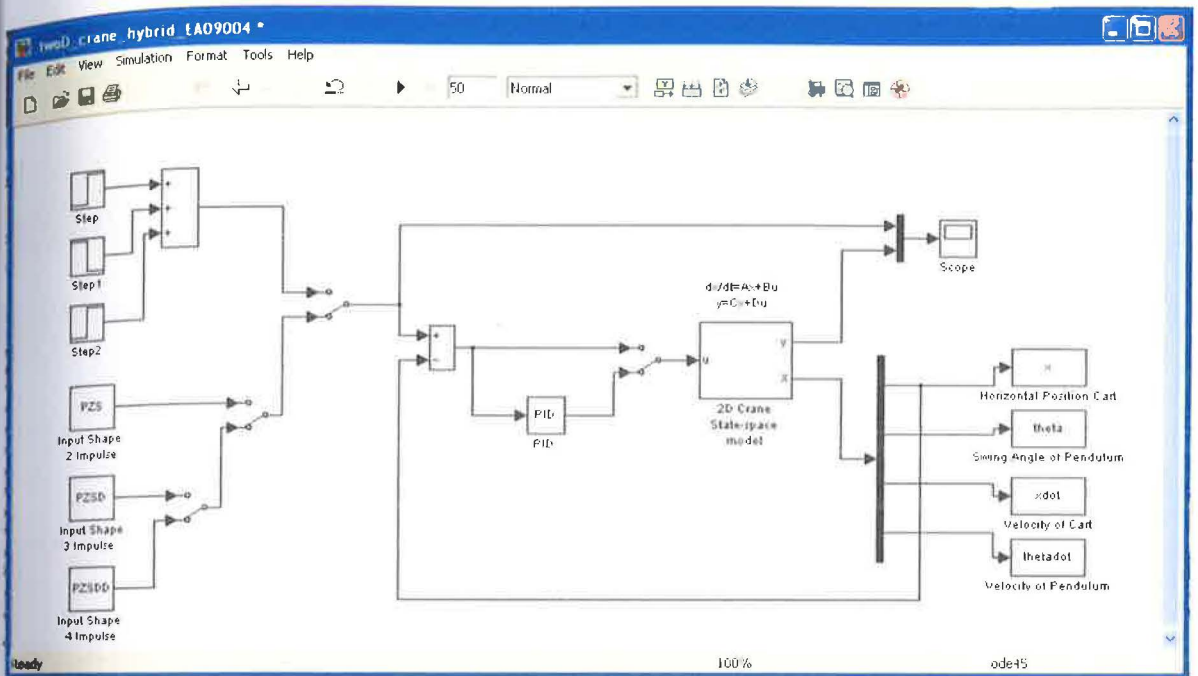


Figure 4.1: A block diagram design of a gantry crane system in MATLAB

4.3.1 Simulation result without controller

Figure 4.2-4.4 shows the response of power spectra density, swing angle of the pendulum and the horizontal position cart of the gantry crane system without using hybrid input shaping and PID controller schemes. These results were considered as the system response of the unshaped bang-bang torque input to evaluate the performance of gantry crane by comparing the result between a simulation design before and after applying controller. These results show that a sway occurred during the movement of the pendulum. The maximum amplitude of sway angle obtained 30.68 dB with the sway

frequency 0.883Hz, while the maximum amplitude of sway angle of the pendulum and horizontal of the cart is ± 0.189 rad and 3 cm respectively.

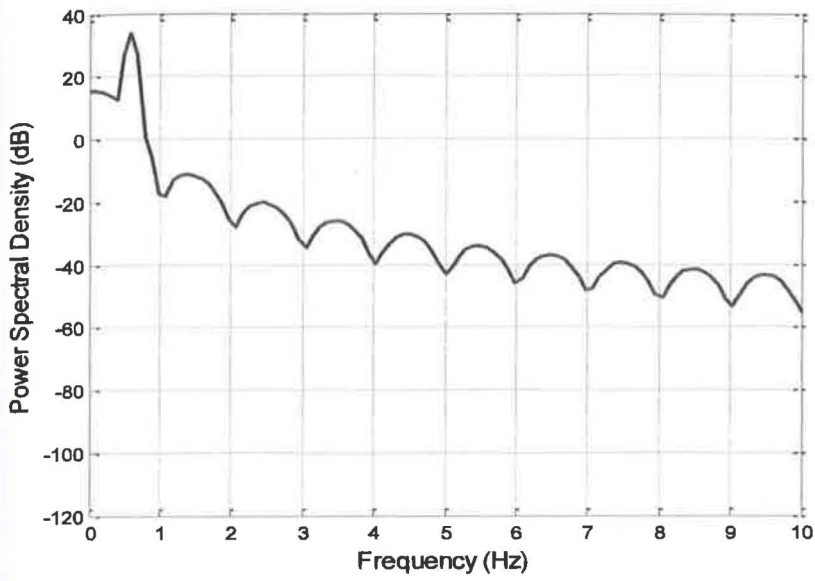


Figure 4.2: Power Spectra Density without Controller

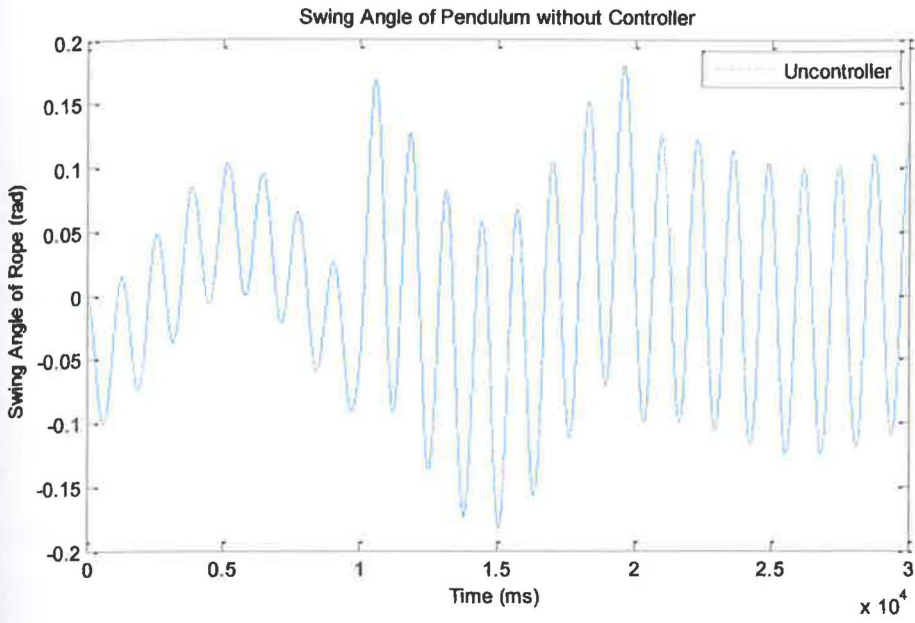


Figure 4.3: Amplitude of sway angle of the pendulum

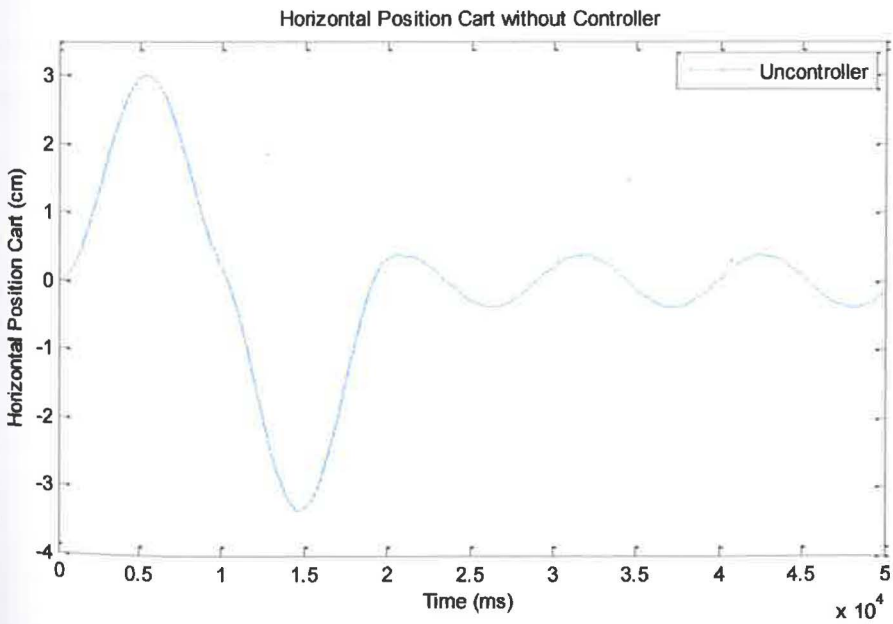


Figure 4.4: Horizontal position of the cart

4.3.2 Determination of Cut-off Frequency

The Cut-off frequency was obtained by simulating a block design in MATLAB with an unfiltered bang-bang torque input. The bang-bang torque command is required in order for the angle of gantry crane position. The first mode of the sway of the system is considered. The responses of the gantry crane system to the unfiltered bang-bang torque input were analyzed in the frequency domain (Spectral density). These results were considered as the system response to the unfiltered input and will be used to evaluate the performance of hybrid input shaping and PID control techniques.

The graph of cutoff frequency is shown in Figure 4.5. Thus, the sway frequency of the gantry crane was obtained at 0.883 Hz for the first mode of sway. A suitable cutoff frequency is half the sway frequency. Since the sway frequency must be higher than the bandwidth of the input signal, a cutoff frequency chosen in this way properly filters out unwanted frequency components. If the cut-off frequency is too high, those components may not be filtered out. If the cut-off frequency is too low, it might narrow the bandwidth of the input signal.

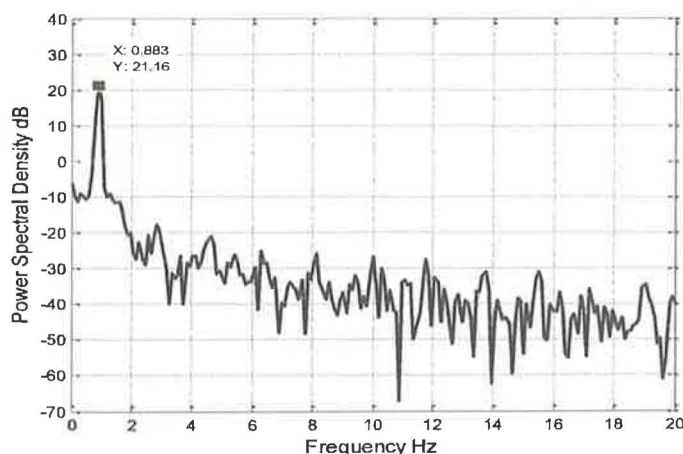


Figure 4.5: Cut-off frequency

4.3.3 The Unshaped Bang – Bang Torque Input Design

The unshaped bang-bang torque input is designed in simulation to determine characteristic parameters of the system and evaluation of the positive input shaping technique including PZS, PZSD and PZSDD as show in Figure 4.6-4.8. A suitable unshaped bang-bang torque will be designed by using a small value of parameter to reduce the amplitudes sway angle of the pendulum. Thus, it will make less vibration of the sway angle and the settling down will becomes longer to obtain a reduction of sway angle of the pendulum with the increment number of impulses in positive input shaping techniques.

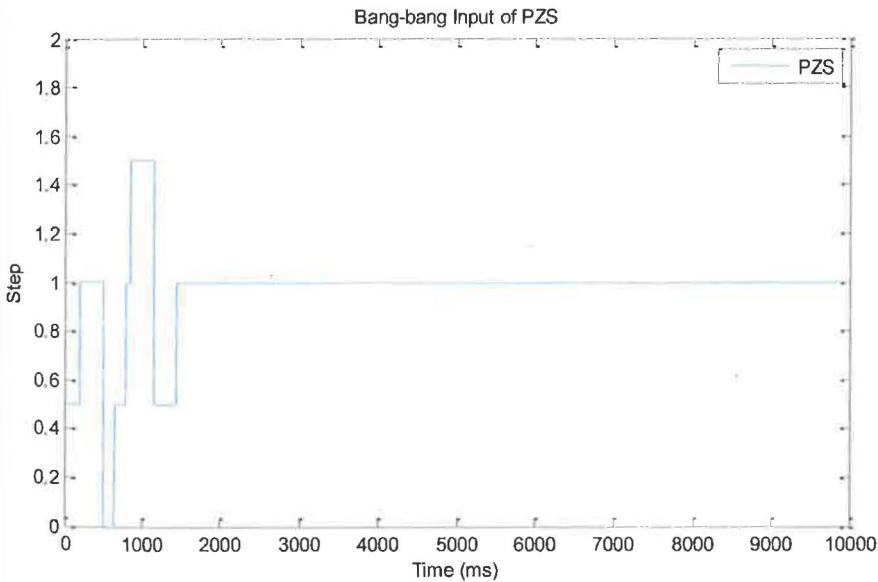


Figure 4.6: Bang-bang Input Torque for PZS

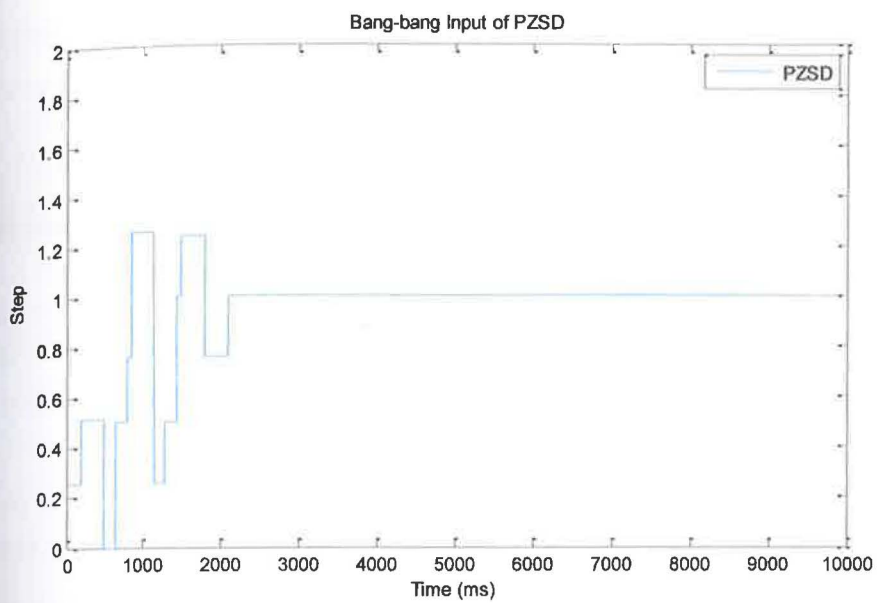


Figure 4.7: Bang-bang Input Torque for PZSD

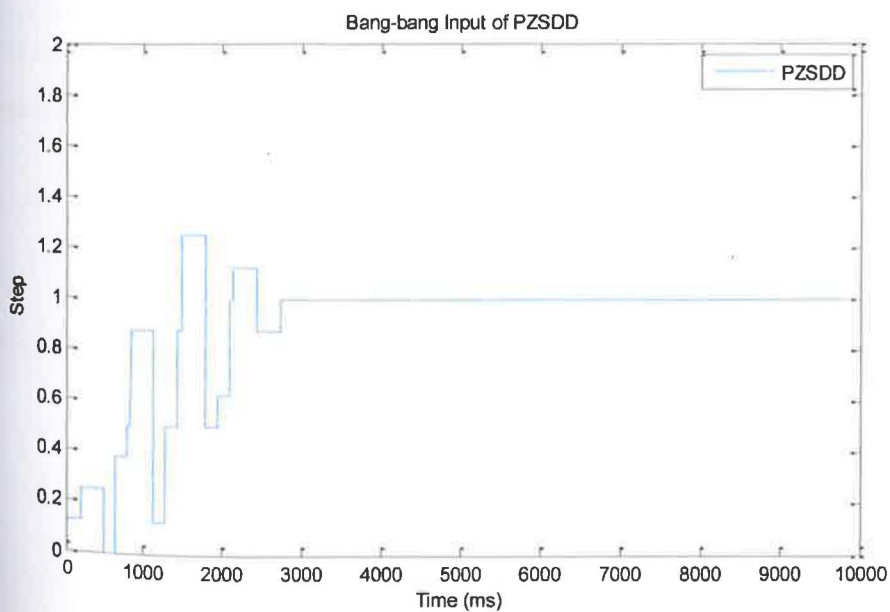


Figure 4.8: Bang-bang Input Torque for PZSDD

4.4 Simulation result with controller based on hybrid input shaping and PID control schemes.

4.4.1 Positive Zero Sway (PZS) and PID Controller

Figure 4.9 to 4.11 show the power spectral density, sway angle of the pendulum and the horizontal position of cart of gantry crane after positive zero sway (PZS) shaper and PID control schemes being applied to the system. These results show the performance of hybrid input shaping and PID control schemes has been developed to reduce the sway angle of the gantry crane. Based on simulation result the level sway reduction of the pendulum in Figure 4.9 shows a slight changed for hybrid PZS shaper and PID control by achieving as much as 2.113 dB. Figure 4.10 shows a maximum reduction in amplitude of sway angle of the pendulum is ± 0.0358 rad compared to Figure 4.3 which produce higher amplitude without using a controller. The response of the cart position shows the time for the pendulum to settling down is 1.5×10^4 ms with zeros overshoot while the rise time is 0.8×10^4 ms.

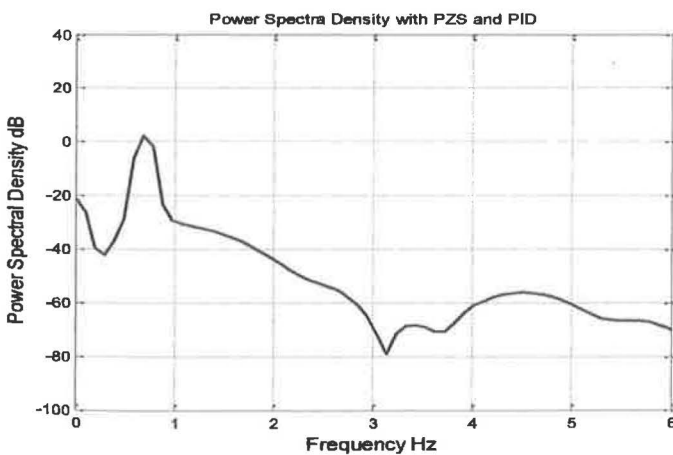


Figure 4.9: Power spectra density PZS and PID

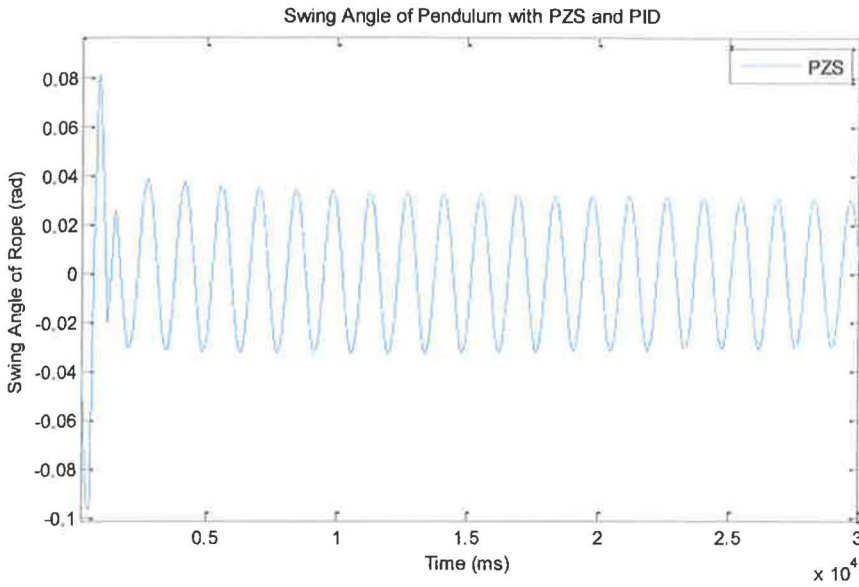


Figure 4.10: Amplitude of sway angle of the pendulum PZS and PID

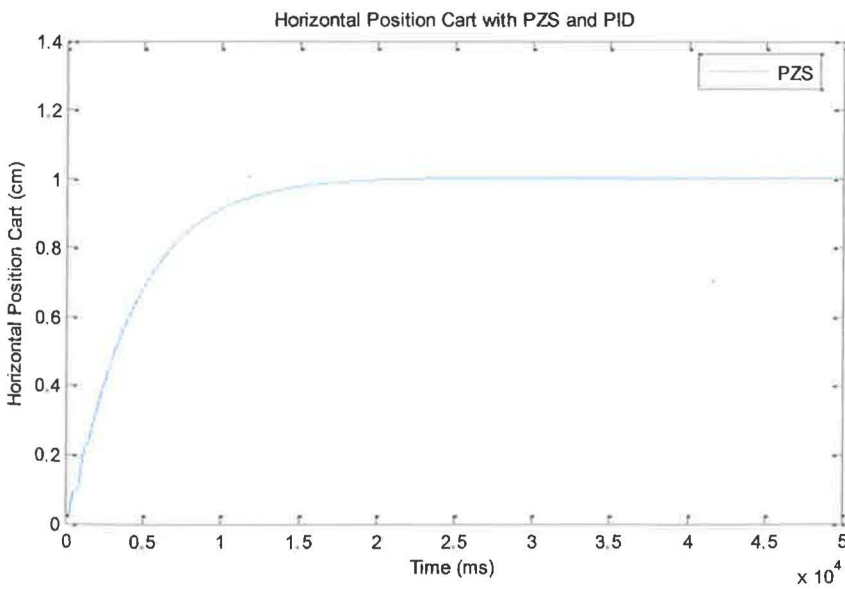


Figure 4.11: Horizontal position of the cart PZS and PID

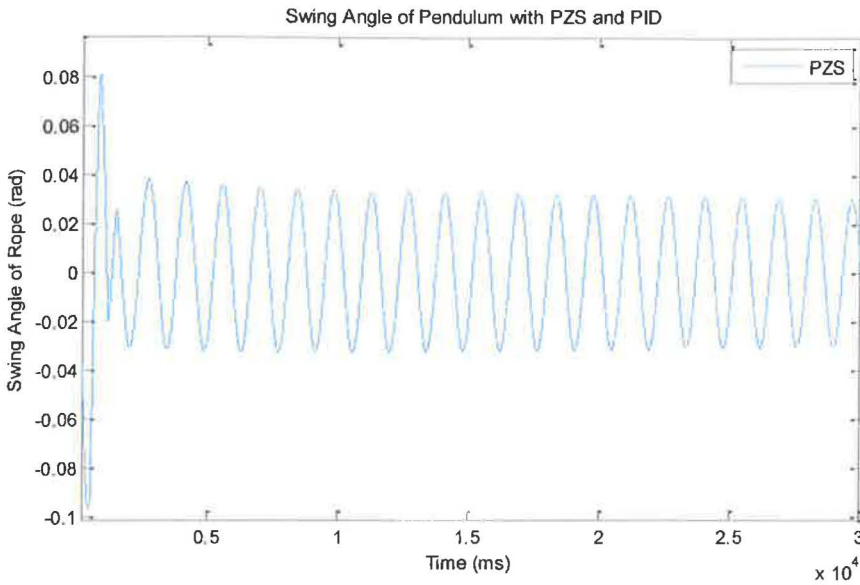


Figure 4.10: Amplitude of sway angle of the pendulum PZS and PID

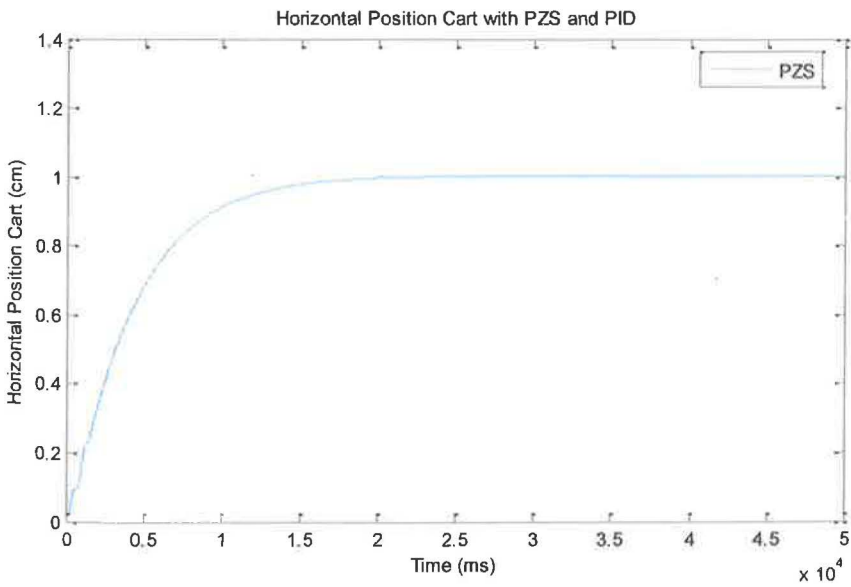


Figure 4.11: Horizontal position of the cart PZS and PID

4.4.2

Positive Zero Derivative (PZSD) and PID Controller Schemes

Figure 4.12 to 4.14 show the power spectral density, sway angle of the pendulum and the horizontal position of the cart of gantry crane after positive zero sway derivative (PZSD) shaper and PID control schemes being applied to the system. When increasing the value of proportional gain (K_p) at 250, integral gain (K_i) at 0.0025 and derivative gain at 1000 the results in Figure 4.12 give an improvement which the levels sway reduction become decreased to -15.08 dB. The maximum amplitude of sway angle of the pendulum also decreased to ± 0.0081 rad in Figure 4.13 while the reading position of the cart in Figure 4.14 increased to 0.9978 cm and achieved time to settling down the movement of the pendulum in 1.52×10^4 ms with zeros overshoot and the rise time was increased to 0.92×10^4 ms respectively.

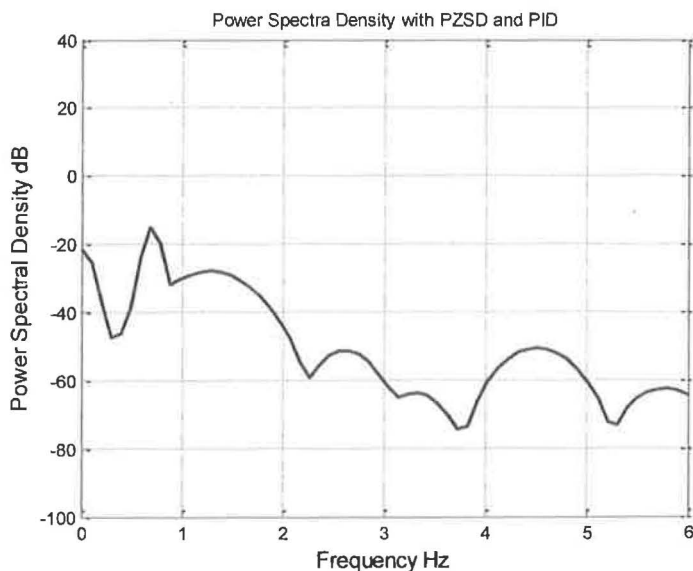


Figure 4.12: Power spectra density PZSD and PID

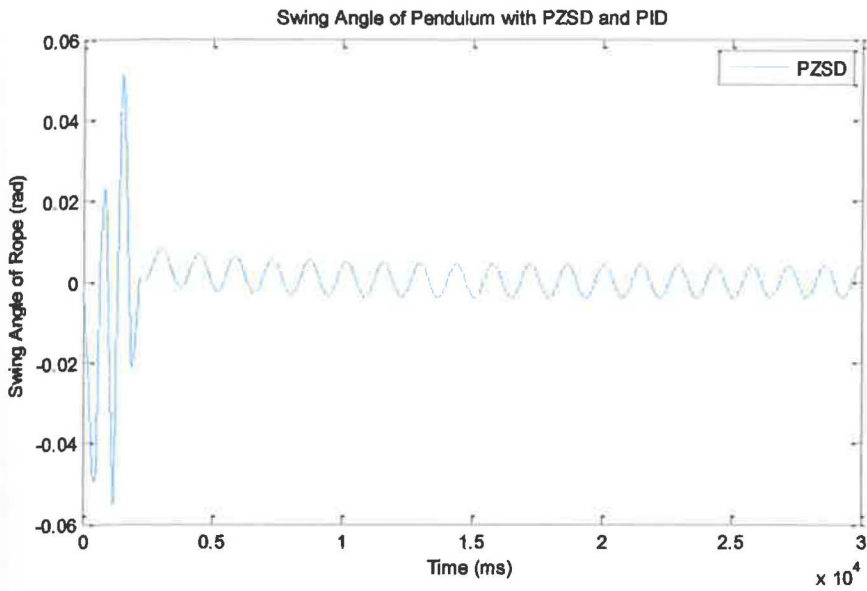


Figure 4.13: Amplitude of sway angle of the pendulum PZSD and PID

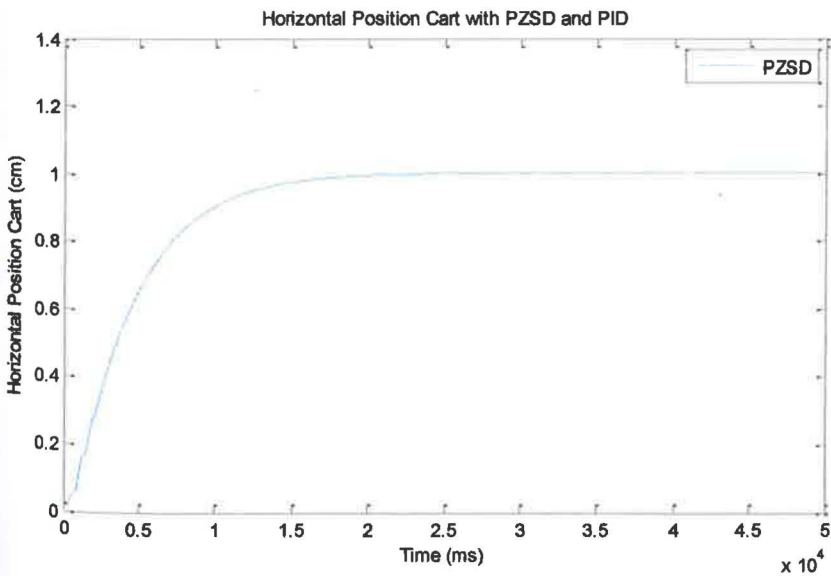


Figure 4.14: Horizontal position of the cart PZSD and PID

4.4.3 Positive Zero Derivative-derivative (PZSDD) and PID Controller

Figure 4.15 to 4.17 show the power spectral density, sway angle of the pendulum and the horizontal position of the cart of gantry crane after positive zero sway derivative-derivative (PZSDD) shaper and PID control schemes being applied to the system. The level of sway reduction in Figure 4.15 shows a better improvement by giving a reading -38.18 dB. It has been proved with reducing amplitude of sway angle of the pendulum at 0.0039 rad in Figure 4.16 while the reading position of the cart in Figure 4.17 increased to 0.9979 cm and achieved time to settling down the movement of the pendulum in 1.54×10^4 ms with zero overshoot and the rise time was increased to 0.94×10^4 ms respectively.

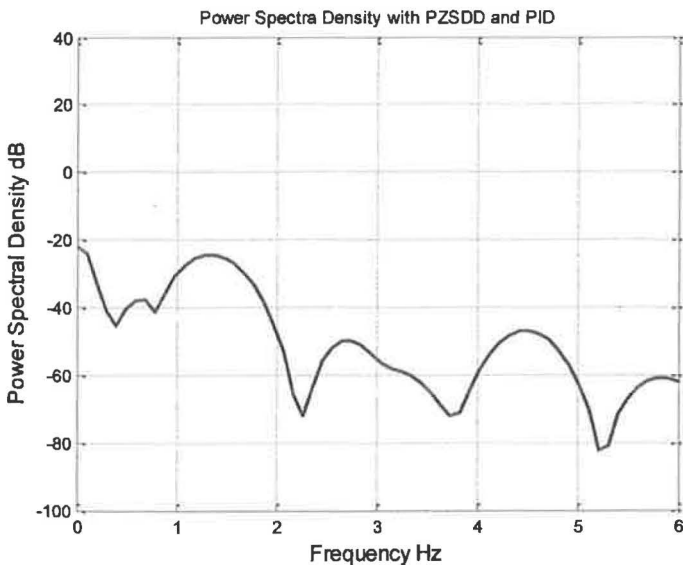


Figure 4.15: Power spectra density PZSDD and PID

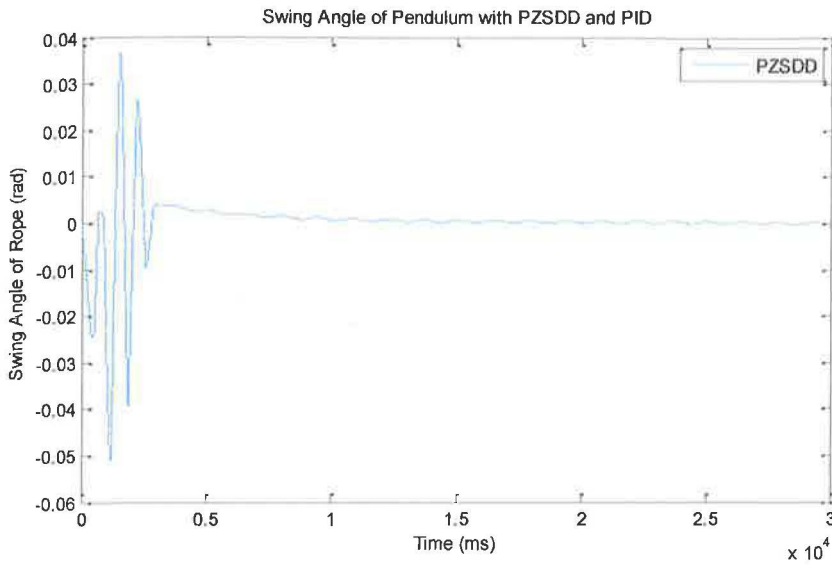


Figure 4.16: Amplitude of sway angle of the pendulum PZSDD and PID

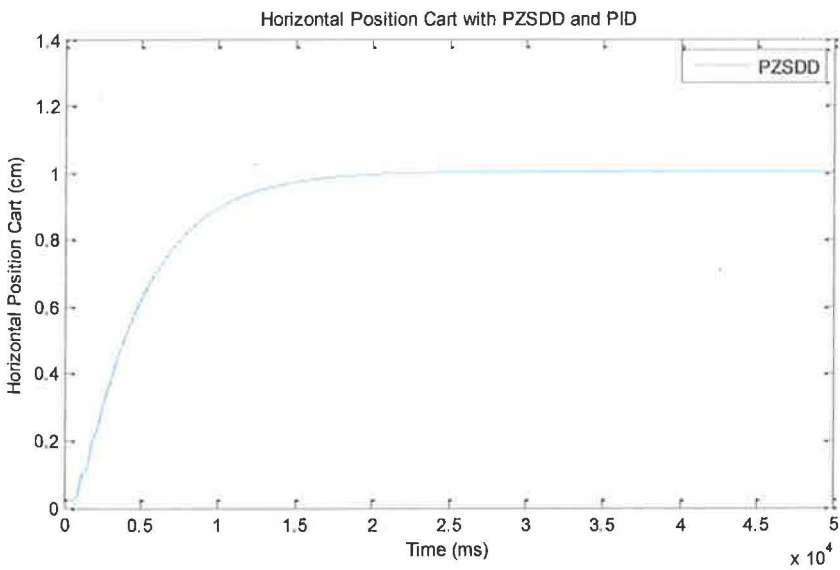


Figure 4.17: Horizontal position of the cart PZSDD and PID

4.5 Comparison in Simulation Result

4.5.1 Comparison of Power Spectra Density

Figure 4.18 shows the comparison of power spectra density (PSD) between hybrid PID control schemes with PZS, PZSD and PZSDD shaper in the simulation result. The attenuation of the level of sway angle data in power spectra density was analyzed of each type of shaper. Based on a comparison result from the PSD of the sway angle response, the swaying frequencies are dominated by the first mode, which are obtained as 0.6868 Hz, 0.6868 Hz and 0.5887 Hz with a magnitude of 2.113 dB, -15.08 dB and -38.18 dB for the hybrid PID control schemes with PZS, PZSD and PZSDD shaper respectively as shows in Table 4.1.

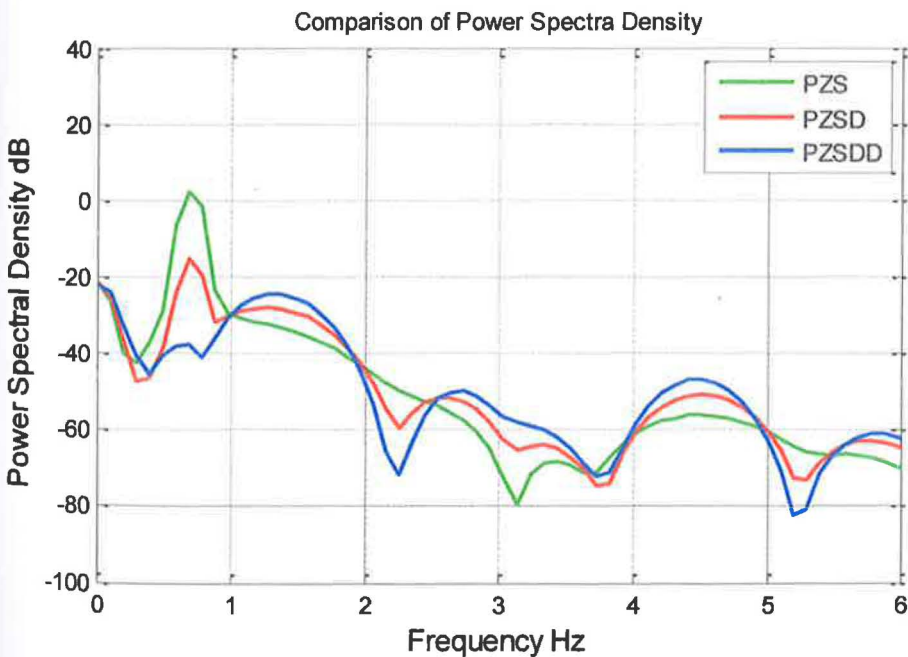


Figure 4.18: Comparison of Power Spectra Density

Table 4.1: Response of Power Spectra Density after applying controller

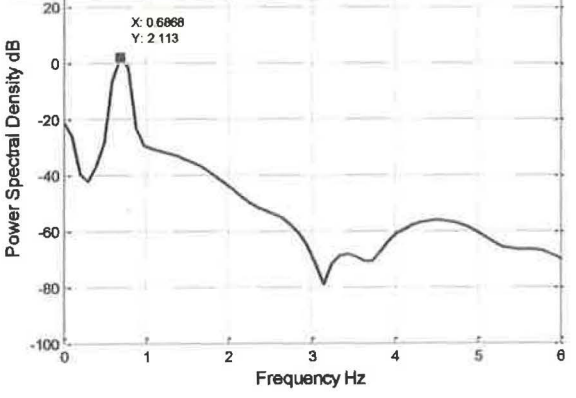
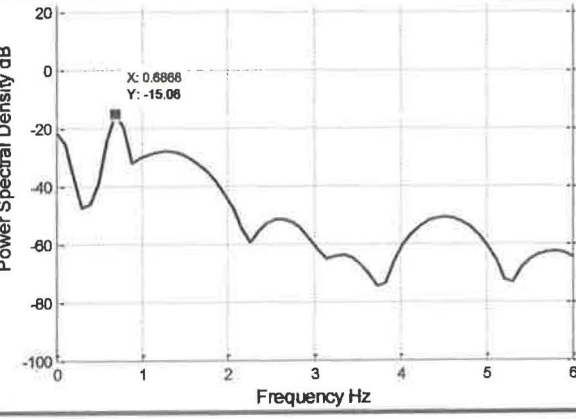
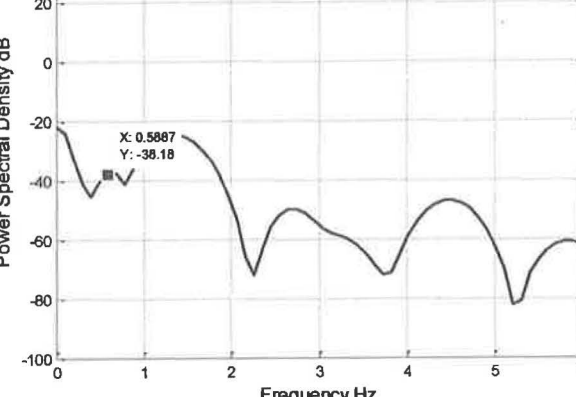
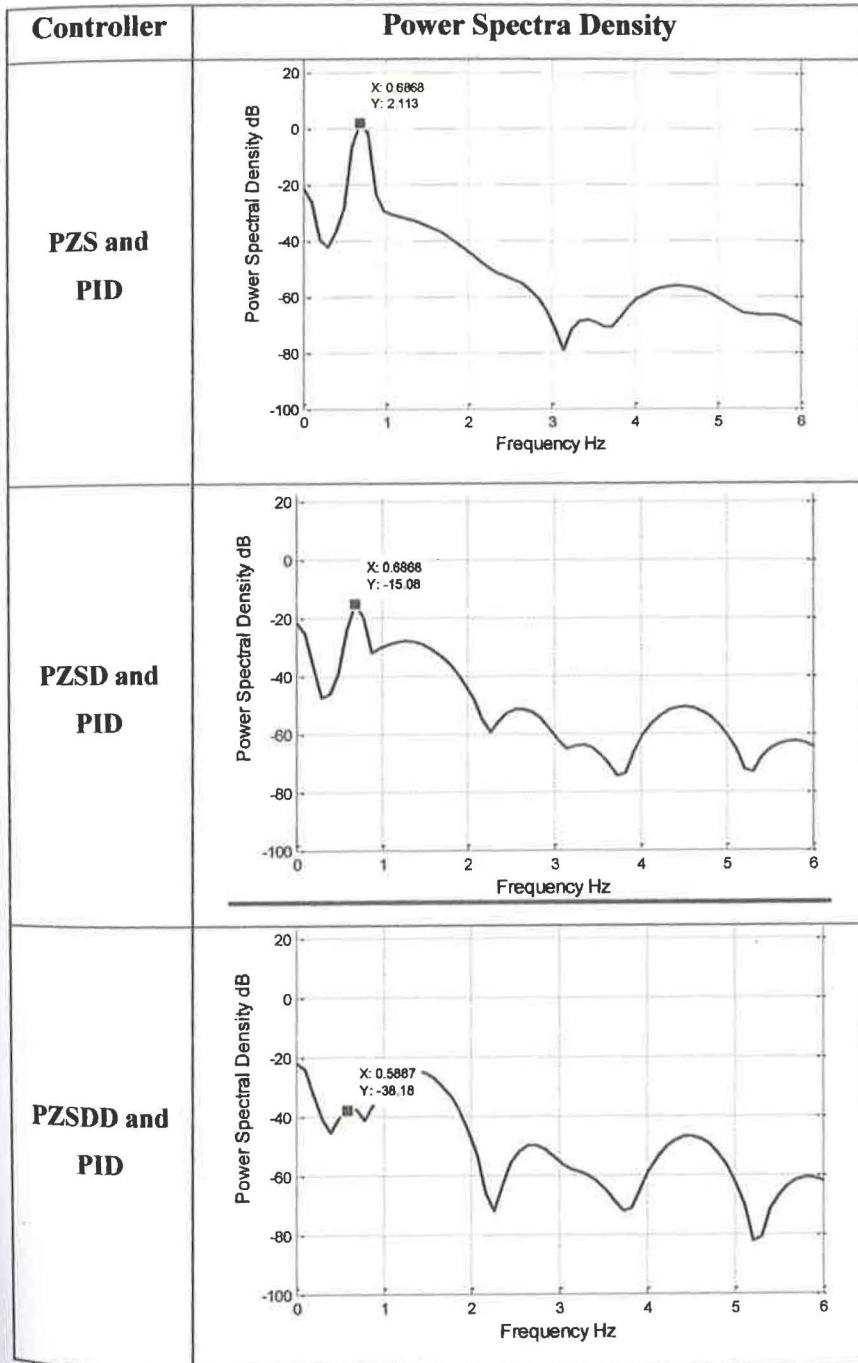
Controller	Power Spectra Density
<p style="text-align: center;">PZS and PID</p>	 <p>Power Spectral Density dB</p> <p>Frequency Hz</p> <p>X: 0.6868 Y: 2.113</p>
<p style="text-align: center;">PZSD and PID</p>	 <p>Power Spectral Density dB</p> <p>Frequency Hz</p> <p>X: 0.6868 Y: -15.06</p>
<p style="text-align: center;">PZSDD and PID</p>	 <p>Power Spectral Density dB</p> <p>Frequency Hz</p> <p>X: 0.5887 Y: -38.18</p>

Table 4.1: Response of Power Spectra Density after applying controller



4.5.2 Comparison of Sway Angle of the Pendulum

Figure 4.19 shows the comparison of sway angle of the pendulum between hybrid PID control schemes with PZS, PZSD and PZSDD shaper in the simulation result. Based on comparison result, it shows that the level of sway angle was significantly reduced with the increasing of positive input shaping derivative order. This is evidenced in the pendulum sway angle responses. The magnitude of sway angle was achieved as ± 0.0358 rad, ± 0.0081 rad and ± 0.0039 rad for the hybrid PID control schemes with PZS, PZSD and PZSDD shaper respectively as shows in Table 4.2.

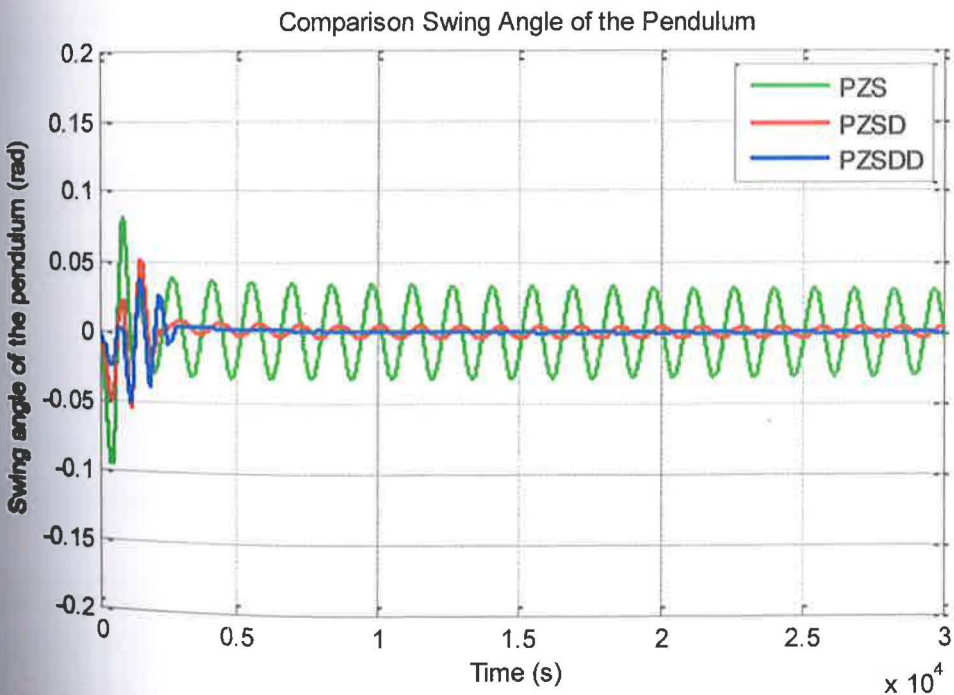
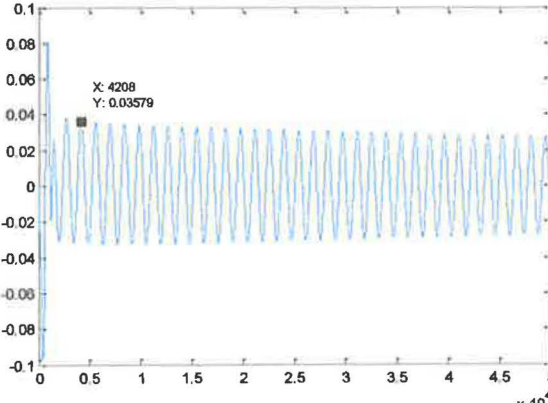
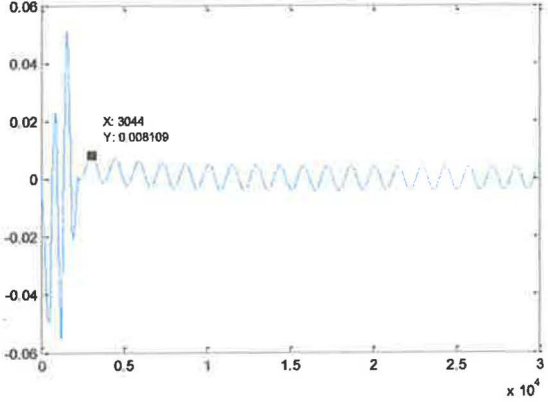
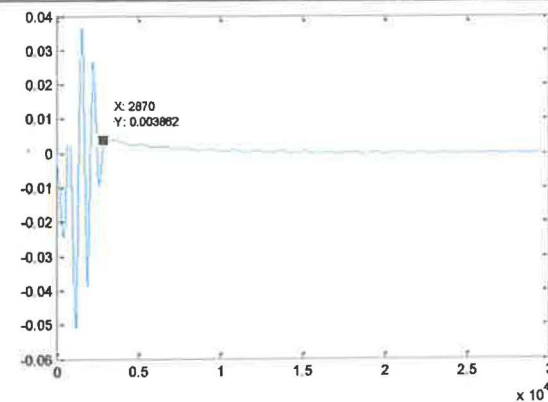


Figure 4.19: Comparison response of sway angle of pendulum

Table 4.2: Response of Swing Angle of Pendulum after applying controller

Controller	Swing Angle of Pendulum
<p>PZS and PID</p>	
<p>PZSD and PID</p>	
<p>PZSDD and PID</p>	

By comparing the result presented in Table 4.3, it is noted the highest performance in the reduction of the sway of the system is achieved using hybrid input shaping based on a PZSDD shaper with PID control schemes. This is observed and compared to hybrid input shaping based on PZS and PZSDD shaper with PID control schemes at the first mode of sway. For comparative assessment, the level of sway reduction of the sway angle of the pendulum using hybrid input shaping and PID control schemes is shown in Figure 4.20. The result shows that, highest level of sway reduction is achieved using PZSDD with PID control schemes followed by PZSD and PZS with PID control schemes. Therefore, it can be concluded the combination feed-forward and feedback controller based on hybrid input shaping and PID control schemes provide better performance in sway reduction as compared to the uncontrolled techniques in the overall.

Table 4.3: Level sway reduction of the single pendulum

Feedback Controller	Feed-forward Controller	Attenuation (dB) of sway of the pendulum	Amplitude of sway angle of the pendulum (rad)
Uncontrolled		30.68	± 0.187
PID	PZS	2.113	± 0.0358
	PSDD	-15.08	± 0.0081
	PZSDD	-38.18	± 0.0039

By comparing the result presented in Table 4.3, it is noted the highest performance in the reduction of the sway of the system is achieved using hybrid input shaping based on a PZSDD shaper with PID control schemes. This is observed and compared to hybrid input shaping based on PZS and PZSDD shaper with PID control schemes at the first mode of sway. For comparative assessment, the level of sway reduction of the sway angle of the pendulum using hybrid input shaping and PID control schemes is shown in Figure 4.20. The result shows that, highest level of sway reduction is achieved using PZSDD with PID control schemes followed by PZSD and PZS with PID control schemes. Therefore, it can be concluded the combination feed-forward and feedback controller based on hybrid input shaping and PID control schemes provide better performance in sway reduction as compared to the uncontrolled techniques in the overall.

Table 4.3: Level sway reduction of the single pendulum

Feedback Controller	Feed-forward Controller	Attenuation (dB) of sway of the pendulum	Amplitude of sway angle of the pendulum (rad)
Uncontrolled		30.68	± 0.187
PID	PZS	2.113	± 0.0358
	PSDD	-15.08	± 0.0081
	PZSDD	-38.18	± 0.0039

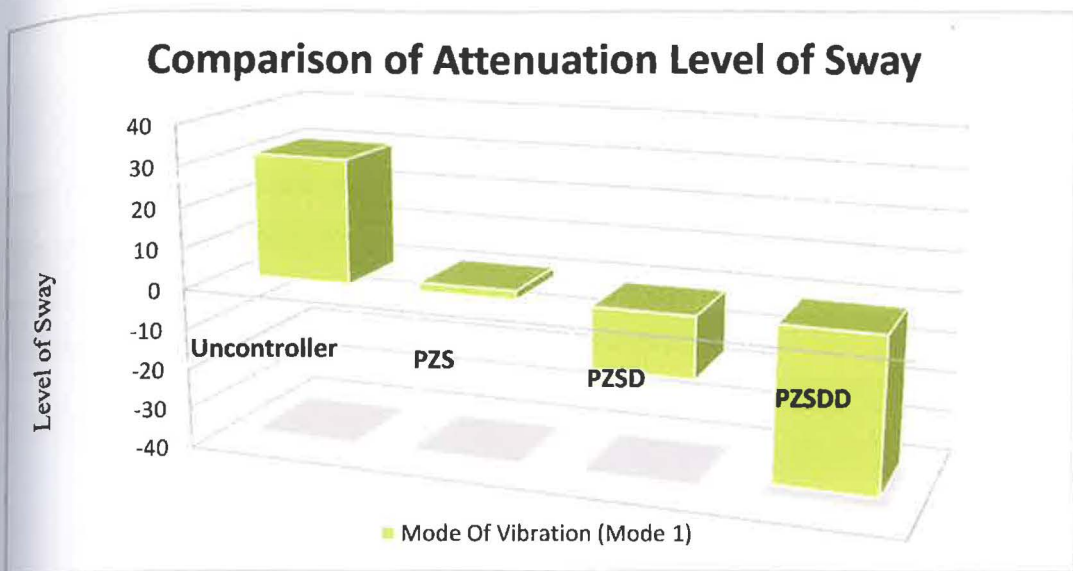


Figure 4.20: Level of Sway Reduction

4.5.3 Comparison of Horizontal Position Cart

Figure 4.21 shows the comparison of the horizontal position cart between hybrid PID control schemes with PZS, PZSD and PZSDD shaper in the simulation result. Based on comparison result, the position of the trolley keeps reducing with higher derivative order of positive input shaping. Therefore, the speed of the system was reduced by the increasing number of impulse sequence.

The corresponding rise time, settling time and overshoot of the trolley position response is depicted in Table 4.4. Using the hybrid PID control schemes with PZS shapes, the cart motion is more faster than PZSD and PZSDD shaper. However, there is no overshoot in the responses of the cart motion for all hybrid input shaping and PID control cases.

The settling time and rise time of the cart position response by using the PZS shaper with PID control schemes is smaller than using the PZSD or PZSDD shaper with PID control schemes which are 1.50×10^4 ms follow by 1.52×10^4 ms and 1.54×10^4 ms for settling time while for the rise time is at 0.80×10^4 ms, 0.92×10^4 ms and 0.94×10^4 ms respectively.

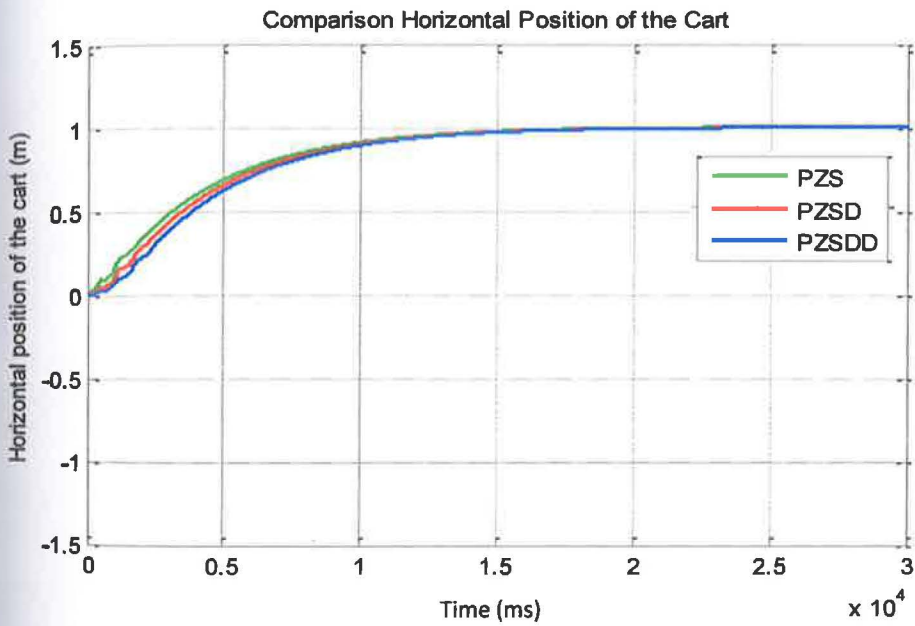
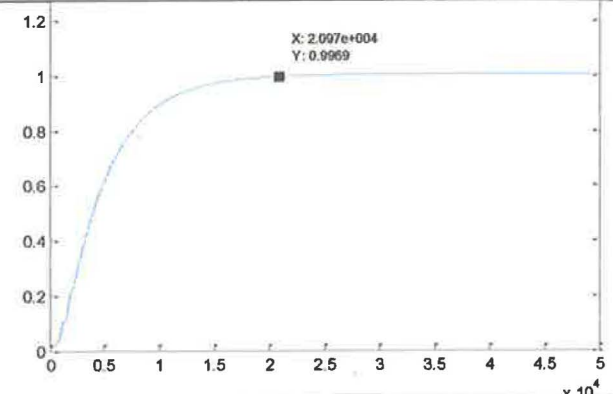
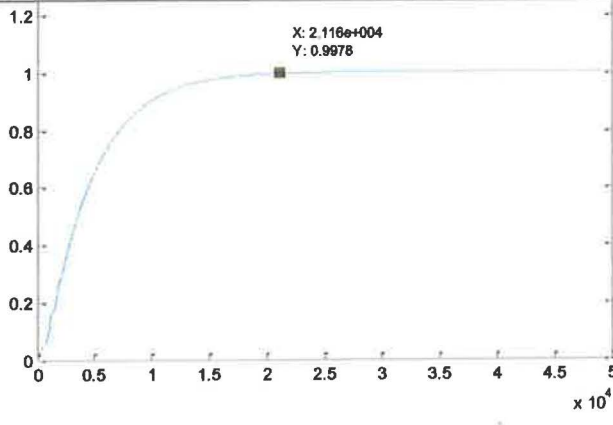
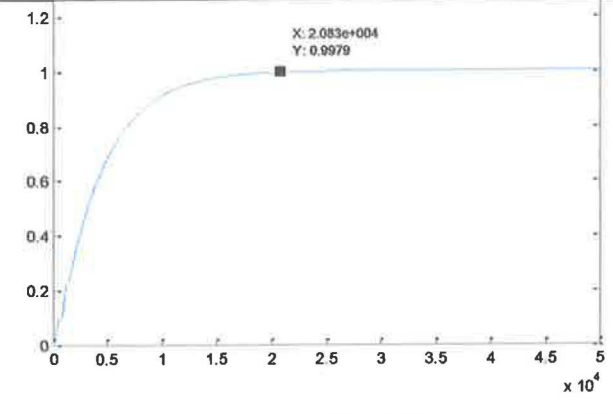


Figure 4.21: Comparison Response of Horizontal Position Cart

Table 4.4: Response of Horizontal position of the cart after applying controller

Controller	Horizontal position of the cart
<p style="text-align: center;">PZS and PID</p>	 <p style="text-align: center;">X: 2.097e+004 Y: 0.9969</p>
<p style="text-align: center;">PZSD and PID</p>	 <p style="text-align: center;">X: 2.116e+004 Y: 0.9978</p>
<p style="text-align: center;">PZSDD and PID</p>	 <p style="text-align: center;">X: 2.083e+004 Y: 0.9979</p>

The time response specifications of rise time, settling time and overshoot of the cart position response for hybrid input shaping and PID control schemes are depicted in Table 4.5. Based on Figure 4.21, it is noted that a slower cart position response before and after using controller was achieved. It is shown that, by incorporating more number of impulses in input shaping control schemes resulted in a slower response. Comparison of the response specification of the cart's position response of hybrid input shaping and PID control schemes is summarized in Figure 4.22. It is noted that the settling time of the cart position response by using the PZS shaper with PID control schemes is smaller than using the PZSD or PZSDD shaper with PID control schemes. It shows that the speed of the system response can be improved by using PZS shaper with PID control schemes. It is concluded that the proposed feed-forward and feedback controllers are capable of reducing the system sway while maintaining the steady state position of cart.

Table 4.5: Specification of horizontal position of cart response

Feedback Controller	Feed-forward Controller	Rise Time $\times 10^4$ (s)	Settling Time $\times 10^4$ (s)	Overshoot (%)
PID	PZS	0.80	1.50	0
	PSDD	0.92	1.52	0
	PZSDD	0.94	1.54	0

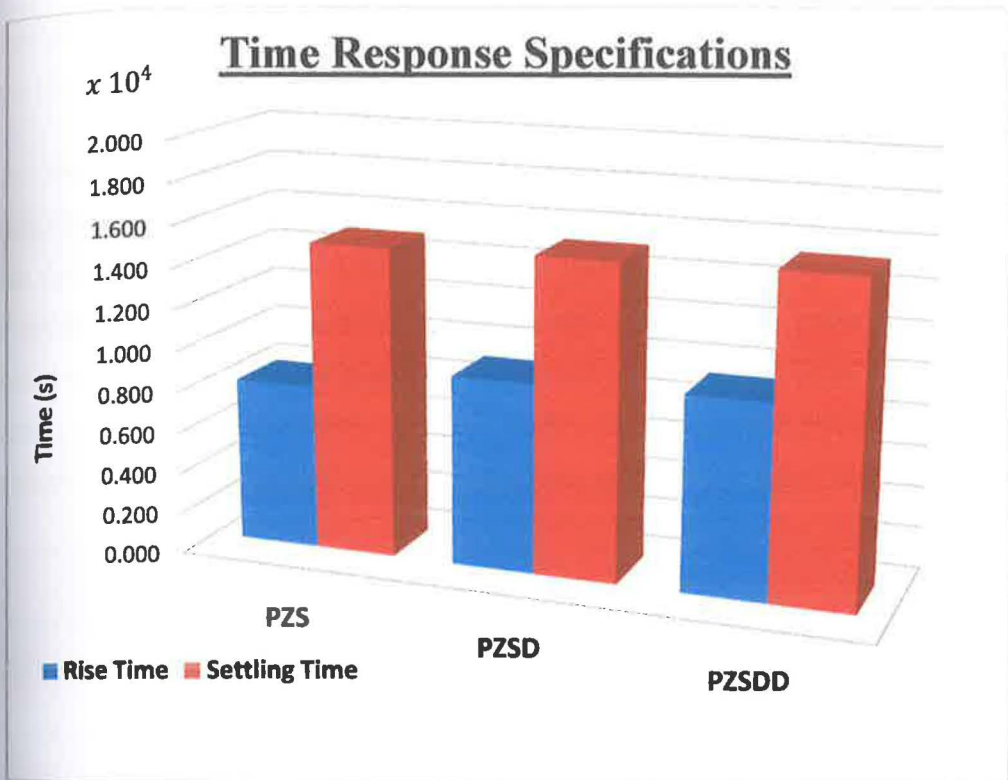


Figure 4.22: Comparison Times Response of the System

4.6 Experimental results using CEM-Tools

In order to verify the effectiveness of the proposed hybrid input shaping and PID schemes, experimental research was conducted on a Real Gain lab-scale gantry crane system, I/O board hardware and CEM-Tools, to achieve the same output as the simulation studies. In this investigation, hybrid input shaping and PID control schemes are implemented and tested with the experimental environment of the lab-scale gantry

crane system and the corresponding results are presented. The bang-bang input voltage of $\pm 10V$ is applied to the cart of the gantry crane system.

To study the effectiveness of sway suppression, PID controller schemes are designed based on the sway frequencies and damping ratios of the gantry crane system. The first mode of the sway of the system is considered, as these dominate the dynamic of the system. The responses of the gantry crane system to the unshaped input were analyzed in time-domain and frequency domain of power spectral density. These results were considered as the system response to the unshaped input and will be used to evaluate the performance of the hybrid input shaping and PID control schemes.

4.6.1 Experiment result without controller

Figure 4.23 show horizontal position of cart of and sway angle of the pendulum of gantry crane without using hybrid input shaping and PID controller schemes. These results were considered as the system response of the unshaped bang-bang torque input to evaluate the performance of gantry crane by comparing the result between experiment design before and after applying controller. The maximum amplitude of sway angle of the pendulum and horizontal of the cart is ± 13.34 rad and 43.24 cm respectively. It is noted that a sway occurred during the movement of the pendulum.

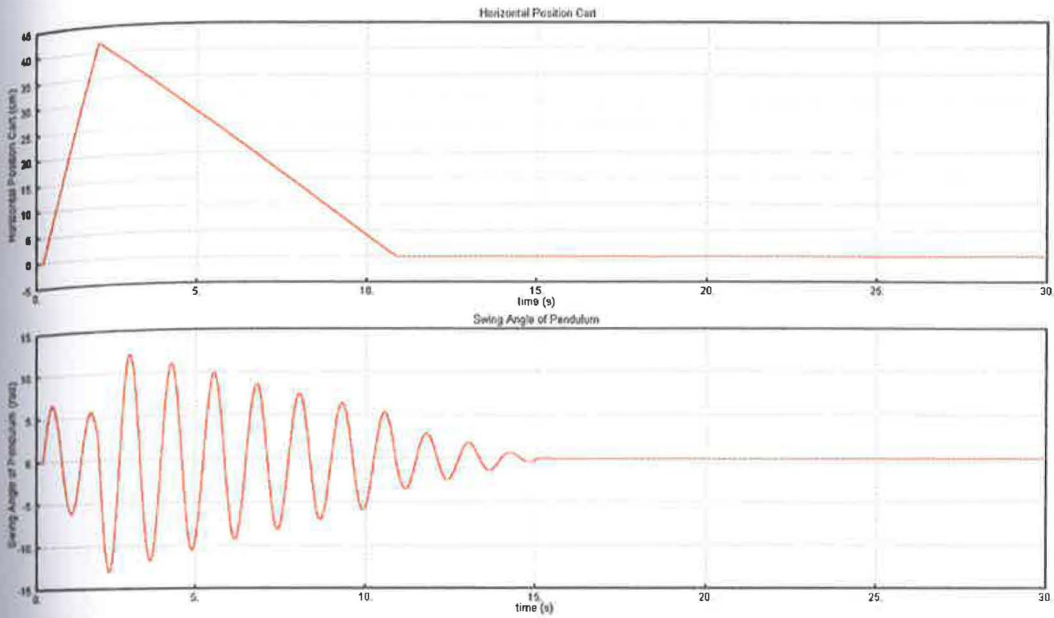
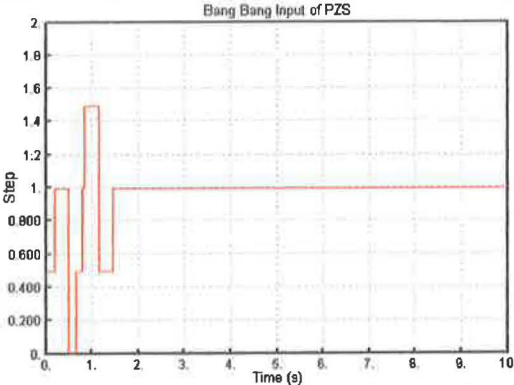
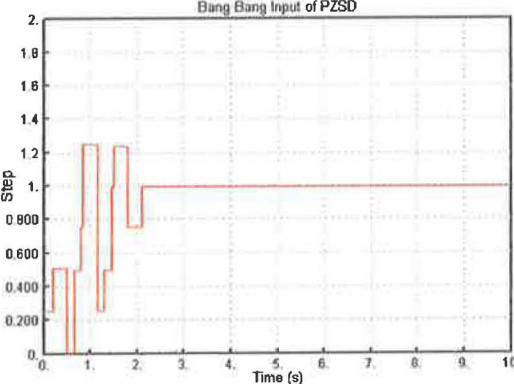
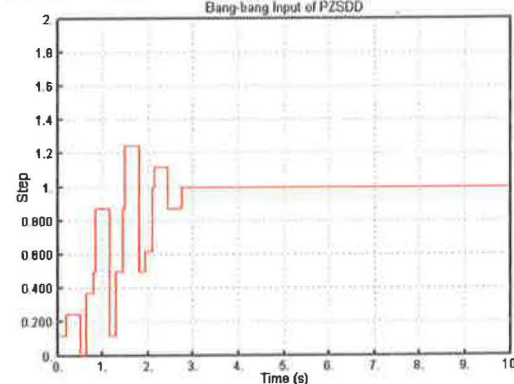


Figure 4.23: The horizontal position of the cart and sway angle of the pendulum without a controller

4.6.2 Bang – Bang Torque Input Design

The bang-bang input torque of input shaping were generated through the convolution of its impulse. Table 4.6 shows the bang-bang input of positive input shaping based on PZS, PZSD and PZSDD shaper in experimental result.

Table 4.6: The bang-bang input of positive input shaping in experimental result.

Bang-bang Torque	Techniques Input Shaping
<p data-bbox="124 629 372 700">Positive Zero Sway (PZS)</p>	 <p data-bbox="638 482 789 503">Bang Bang Input of PZS</p> <p data-bbox="436 503 949 866">A line graph showing the bang-bang input for PZS. The y-axis is labeled 'Step' and ranges from 0 to 2.0 in increments of 0.200. The x-axis is labeled 'Time (s)' and ranges from 0 to 10.0 in increments of 1.0. The input starts at 0, jumps to 1.0 at approximately 0.2s, then to 1.5 at 0.5s, then to 1.0 at 1.0s, and finally settles at 1.0 from 2.0s onwards.</p>
<p data-bbox="124 1038 372 1147">Positive Zero Sway Derivative (PZSD)</p>	 <p data-bbox="638 882 789 903">Bang Bang Input of PZSD</p> <p data-bbox="436 903 949 1265">A line graph showing the bang-bang input for PZSD. The y-axis is labeled 'Step' and ranges from 0 to 2.0 in increments of 0.200. The x-axis is labeled 'Time (s)' and ranges from 0 to 10.0 in increments of 1.0. The input starts at 0, jumps to 0.5 at 0.2s, then to 1.25 at 0.5s, then to 1.25 at 1.0s, then to 0.75 at 1.5s, and finally settles at 1.0 from 2.0s onwards.</p>
<p data-bbox="124 1452 372 1597">Positive Zero Sway Derivative- Derivative (PZSDD)</p>	 <p data-bbox="638 1311 789 1332">Bang-bang Input of PZSDD</p> <p data-bbox="436 1332 949 1694">A line graph showing the bang-bang input for PZSDD. The y-axis is labeled 'Step' and ranges from 0 to 2.0 in increments of 0.200. The x-axis is labeled 'Time (s)' and ranges from 0 to 10.0 in increments of 1.0. The input starts at 0, jumps to 0.25 at 0.2s, then to 0.9 at 0.5s, then to 1.25 at 1.0s, then to 1.1 at 1.5s, then to 1.0 at 2.0s, and finally settles at 1.0 from 3.0s onwards.</p>

4.6.3 Experiment result with controller based on PID control schemes

Figure 4.24 to 4.26 shows the horizontal position of cart of and sway angle of the pendulum of gantry crane after PID control schemes being applied to the system. In this experiment, the value between proportional gains (K_p), integral gain (K_i) and derivative gain (k_d) are compared in respectively.

The level sway reduction of the pendulum in Figure 4.24 shows a highest reduction in amplitude of sway angle of the pendulum is equal to ± 5 rad compared to Figure 4.25 and Figure 4.26 which produce lowest reduction of amplitude at ± 14.8 rad and ± 16.5 rad since the energy is transferred through the pendulum and also considering the gravitational effect. It is noted that the highest value of Proportional ($P=350$), Integral ($I=385$) and Derivative ($D=90$) as shown in Figure 4.24 may produce a good result in term of sway reduction compared to the smallest value of PID modes at $P=345$, $I=385$ and $D=84$ as show in Figure 4.25 and at $P=320$, $I=0.3$ and $D=15$ as show in Figure 4.26.

In terms of overshoot, settling time, rise time and steady state error of the horizontal position cart showed that the response of the system at Figure 4.25 may produce a good result, with no overshoot, fast rise time and no steady state error compare to the response at Figure 4.24 and Figure 4.26. Based on Figure 4.24 the response of PID modes at $P=350$, $I=385$ and $D=90$, may produce highest overshoot and settling time, slower rise time with zero steady state error while in Figure 4.26 the response of PID modes at $P=320$, $I=0.3$ and $D=15$, may produced lowest overshoot and settling time and had a small effect on the rise time and steady state error.

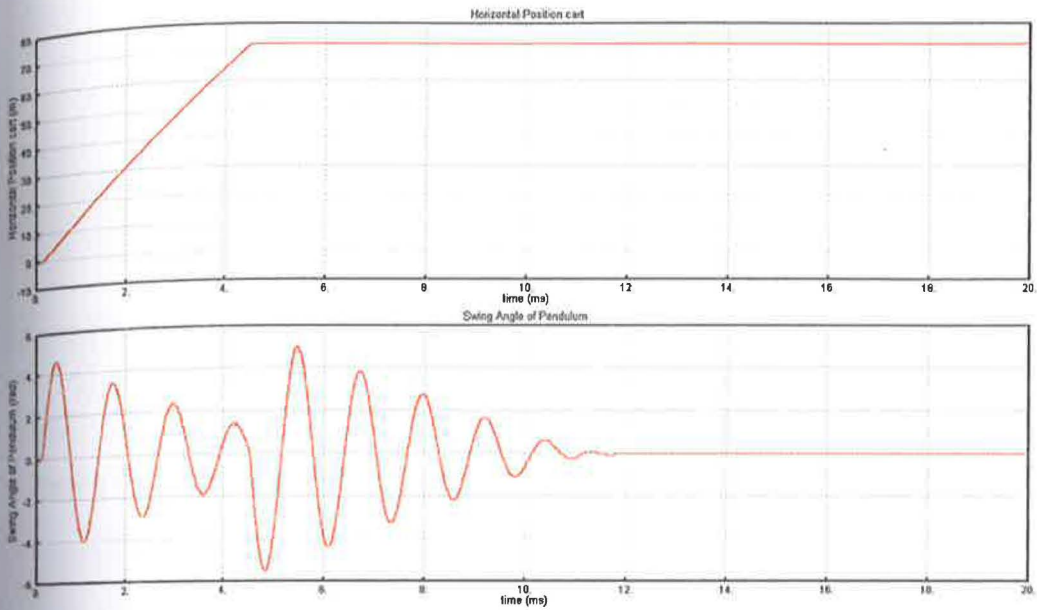


Figure 4.24: The horizontal position of the cart and sway angle of the pendulum at $P=350$, $I=385$ and $D=90$

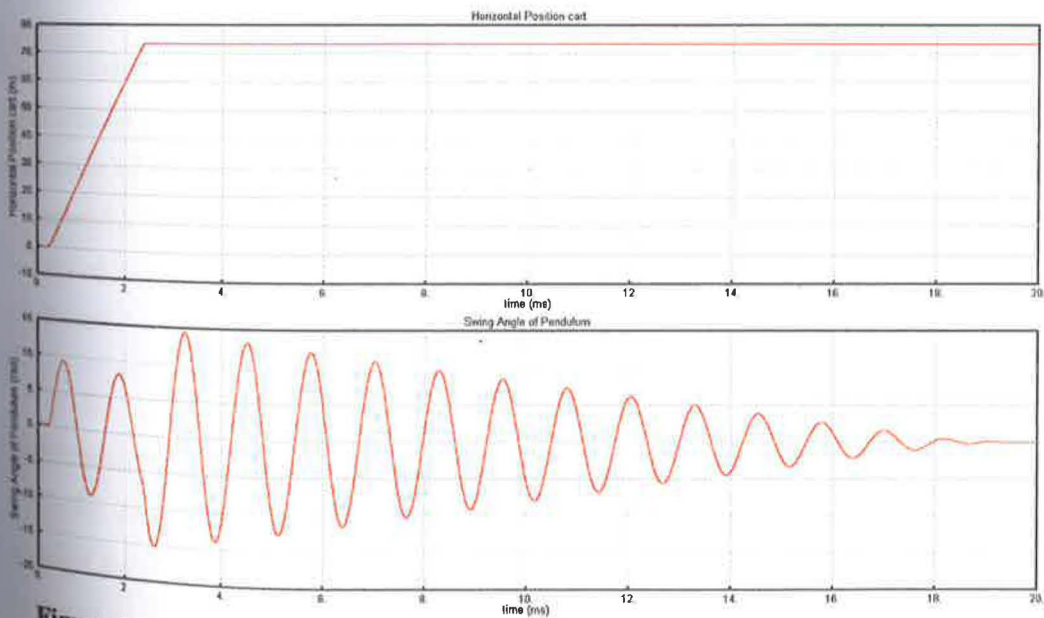


Figure 4.25: The horizontal position of the cart and sway angle of the pendulum at $P=345$, $I=385$ and $D=84$

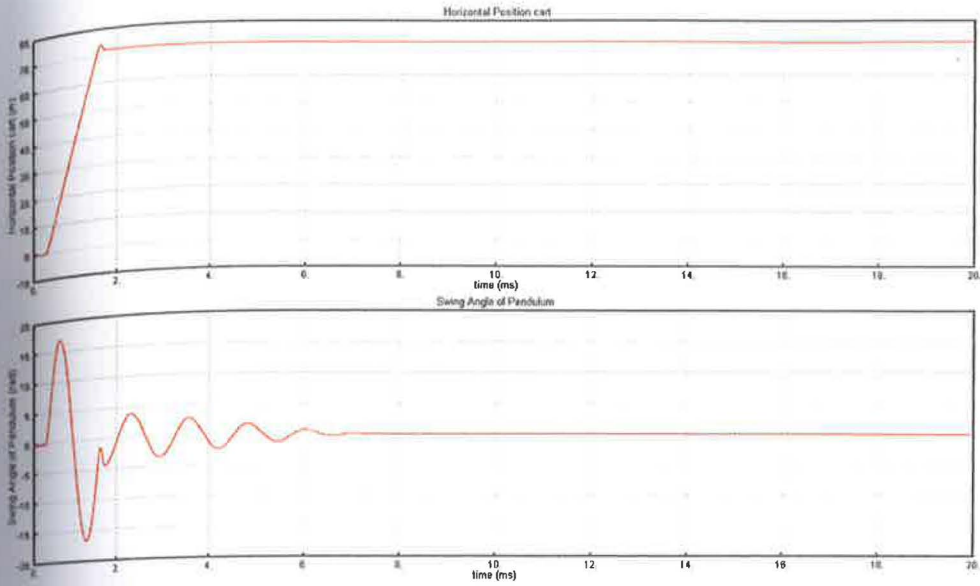


Figure 4.26: The horizontal position of the cart and sway angle of the pendulum at $P=320$, $I=0.3$ and $D=15$

4.7 Experimental Result Analysis

Table 4.7 summarizes the levels of sway reduction of the system responses with and without controller at the first mode. For comparative assessment, the level of sway reduction of the sway angle of the pendulum using PID control scheme is shown in Figure 4.27. The result shows that, highest level of sway reduction is achieved using the values of PID modes at $P=350$, $I=385$, $D=90$ followed by the values at $P=345$, $I=385$, $D=84$ and the values at $P=320$, $I=0.3$, $D=15$.

By comparing the result presented in Table 4.7, it is noted the highest performance in the reduction of sway is achieved using PID control scheme. The value of K_p for Ziegler Nichols Second Method has considered appropriate since too high value of the K_p may cause a degraded system in term of stability. The value of K_i must be tuned in a small value, since an increasing value of I gain tends to increase the settling time of the position cart of gantry crane. Moreover, it might increase the

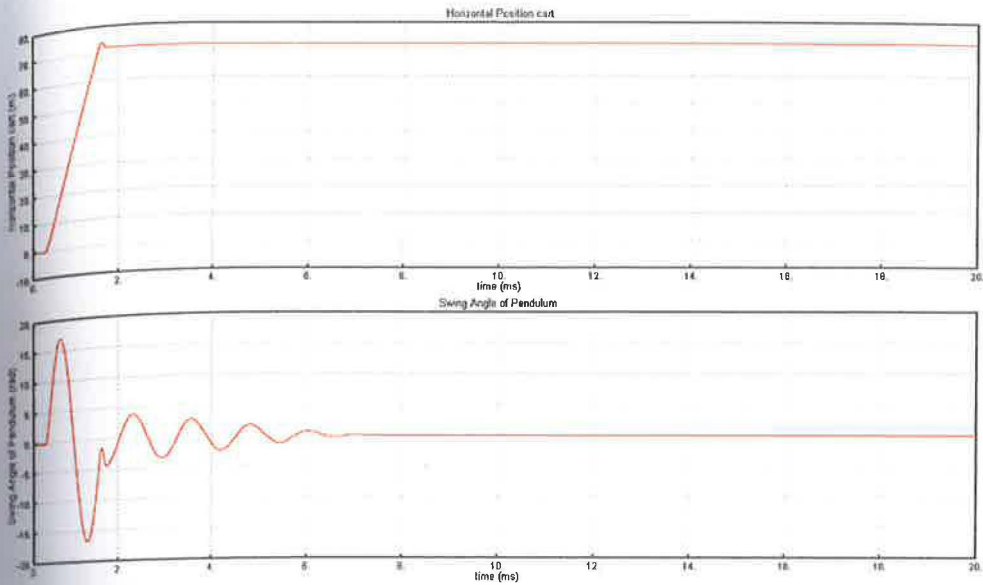


Figure 4.26: The horizontal position of the cart and sway angle of the pendulum at $P=320$, $I=0.3$ and $D=15$

4.7 Experimental Result Analysis

Table 4.7 summarizes the levels of sway reduction of the system responses with and without controller at the first mode. For comparative assessment, the level of sway reduction of the sway angle of the pendulum using PID control scheme is shown in Figure 4.27. The result shows that, highest level of sway reduction is achieved using the values of PID modes at $P=350$, $I=385$, $D=90$ followed by the values at $P=345$, $I=385$, $D=84$ and the values at $P=320$, $I=0.3$, $D=15$.

By comparing the result presented in Table 4.7, it is noted the highest performance in the reduction of sway is achieved using PID control scheme. The value of K_p for Ziegler Nichols Second Method has considered appropriate since too high value of the K_p may cause a degraded system in term of stability. The value of K_i must be tuned in a small value, since an increasing value of I gain tends to increase the settling time of the position cart of gantry crane. Moreover, it might increase the

overshoot and degrade the stability of the system. By increasing the value of K_d , the rise time, settling time and overshoot might decrease in small value, but did not effected the steady state error of the pendulum's sway angle. For a better stability system, the tuned value of K_d must be small.

Table 4.7: Level of sway reduction responses with and without controller

Types Of Controller	Value of each PID mode	Amplitude of sway angle of the pendulum (rad)
Uncontrolled		± 13.34
PID 1	P=350, I=385, D=90	± 5
PID 2	P=345, I=385, D=84	± 14.8
PID 3	P=320, I=0.3, D=15	± 16.5

Comparison Level of Sway Angle of the Single Pendulum

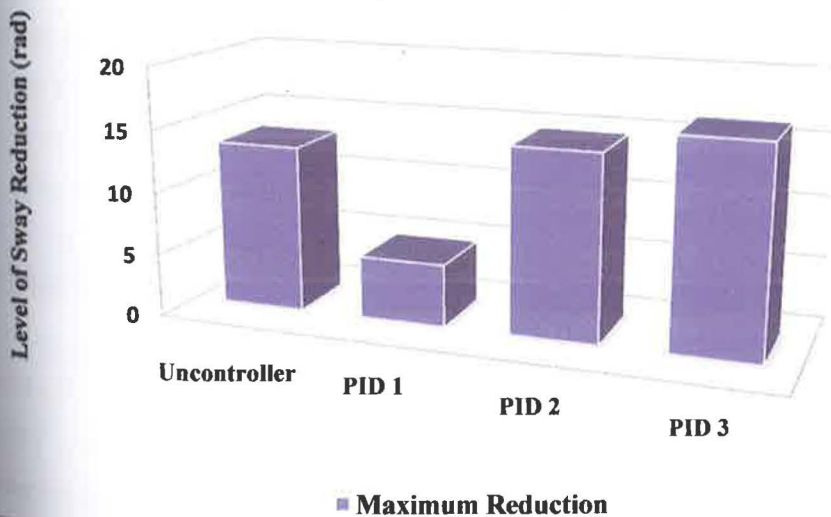


Figure 4.27: Comparison levels of sway reduction with and without controller

CHAPTER 5

CONCLUSION AND RECOMMENDATION

5.1 Conclusion

At the end of this project, active sway control of gantry crane by using hybrid input shaping and PID control schemes has been presented. The objective set in this project to control the sway of the gantry crane system had been implemented and investigated within the lab-scale gantry crane system. In addition, the effects of the difference derivative order of the positive input shaping in term of a level of sway reduction and time response specification have been studied.

The PID gain controller is tuned based on the different parameter specification in order to get the best result. When using an integral control (K_i), it can remove the steady-state error, but worsen the characteristics of the transient response. However the differential proportional gain (K_p) can improve the stability of the system, so it can reduce the overshoot and improve the characteristic of the transient response, while a derivative control (K_d) can increase the stability of the system, reduce the overshoot, and improve the transient response. The comparison result of the specified response of

the cart was investigated with the different value parameters of the initial swing angle position, mass of the loop and the length of the rope.

Moreover the hybrid PID controller and input shaping schemes with higher number of impulses provide a high level of sway reduction. However, in terms of speed of the responses, the input shaping with a low number of impulses, results in a higher speed of tracking response. In overall, the combination feed-forward and feedback controller based on hybrid input shaping and PID control schemes provide better performance in sway reduction as compared to the uncontrolled techniques in the overall.

5.2 Limitation of the Project

In this project the investigation into the hybrid input shaping and PID control schemes are done by using MATLAB and CEM-Tools software. The interfacing connection between CEM-Tools and Gantry Crane Pendulum System are also difficult to set up. The Gantry Crane Pendulum System hardware will react when the block diagram of SIM-Tool start. The cart will swing-up based on the program, however for input shaping schemes data from CEM-Tool have some problem to convert into the workspace of MATLAB. Even though the gantry crane system is modeled using Lagrange-Euler's Method, there is still a difference between the model and actual gantry crane system. Even when applying the technique to Gantry Crane Pendulum System, the result might not be same with the actual system.

Recommendation

Based on this project, there are two recommendations for the future works:

- i. The robust and scale gantry crane is used which is preferable to use in the experiment study.
- ii. For the future application, hybrid input shaping and PID control schemes can be applied to another system which has vibration, to control the position of the cart, since in the real world, the cart position need to be controlled for application purposes.

REFERENCES

- [1] Omar, H.M, Control of gantry and tower cranes. Ph.D. Thesis, M.S. Virginia Tech, 2003.
- [2] Manson, G.A., Time-optimal control of and overhead crane model, *Optimal Control Applications & Methods*, Vol. 3, No. 2, 1992, pp. 115-120.
- [3] Auernig, J. and Troger, H. Time optimal control of overhead cranes with hoisting of the load, *Automatica*, Vol. 23, No. 4, 1987, pp. 437-447.
- [4] Karnopp, B H., Fisher, F.E., and Yoon, B.O., "A strategy for moving mass from one point to another", *Journal of the Franklin Institute*, Vol. 329, 1992, pp. 881-892.
- [5] Teo, C.L., Ong, C. J. and Xu, M. Pulse input sequences for residual vibration reduction. *Journal of Sound and Vibration*, Vol. 211, No. 2, 1998, pp. 157-177.
- [6] Singhose, W.E., Porter L.J. and Seering, W., "Input shaped of a planar gantry crane with hoisting", *Proc. of the American Control Conference*, 1997, pp. 97-100.
- [7] Belanger, N.M., *Control Engineering: A Modern Approach*, Saunders College Publishing, 1995.
- [8] Wahyudi and Jalani, J., Design and implementation of fuzzy logic controller for an intelligent gantry crane system, *Proceedings of the 2nd International Conference on Mechatronics*, 2005, pp. 345- 351.
- [9] Kim, Y.S., Yoshihara, H., Fujioka, N., Kasahara, H., Shim. H., Sul, S.K., A new vision-sensorless anti-sway control system for container cranes, *Industry Applications Conference*, 2003.
- [10] Choi, S.U., Kim, J.H., Lee, J.W., Lee, Y.J., Lee, K.S., "A study on gantry crane control using neural network two degree of PID controller", *Proceedings of the International Symposium on Industrial Electronics*, Pusan, Korea, pp. 1896-1900, 2001.

- [1] Pieper, J.K. and Surgenor, B.W., "Discrete time sliding mode control applied to a gantry crane", Proceedings of the 33rd Conference on Decision and Control Lake Buena Vista, FL, pp. 829-834, December 1994.
- [2] O'Connor, W.J., "Gantry crane control: a novel solution explored and extended", *Proceedings of the American Control Conference*, Anchorage, AK, May 8-10, pp. 250-255, 2002.
- [3] Smith, O.J.M., *Feedback Control Systems*. 1958, New York: McGraw-Hill Book Company, Inc. 33 1-345.
- [4] Starr, G.P., "Swing-Free Transport of Suspended Objects With a Path-Controlled Robot Manipulator," *J. of Dynamic Systems, Measurement and Control*, 107: p. 97-100, 1985.
- [5] Singer, N.C. and W.P. Seering, "Preshaping Command Inputs to Reduce System Vibration," *J. of Dynamic Systems, Measurement, and Control*, 112(March): p. 76-82, 1990.
- [6] Tallman, G.H. and O.J.M. Smith, "Analog Study of Dead- Beat Posicast Control," *IRE Transactions on Automatic Control*, (March): p. 14-21, 1958.
- [7] Singhose, W., W. Seering, and N. Singer, "Residual Vibration Reduction Using Vector Diagrams to Generate Shaped Inputs," *J. of Mechanical Design*, 116(June): p. 654-659, 1994.
- [8] Magee, D.P. and W.J. Book, "Filtering Schilling Manipulator Commands to Prevent Flexible Structure Vibration," *American Control Conf.*, Baltimore, MD, pp. 2538-42, 1994.
- [9] Hillsley, K.L. and S. Yurkovich, "Vibration Control of a Two-Link Flexible Robot Arm," *Journal of Dynamics and Control*, 3, p. 261-280, 1993.
- [20] Feddema, J.T., "Digital Filter Control of Remotely Operated Flexible Robotic Structures," *American Control Conference*, San Francisco, CA, Vol. 3, pp. 2710-2715, 1993.
- [21] Noakes, M.W. and J.F. Jansen, "Generalized Inputs for Damped-Vibration Control of Suspended Payloads," *Robotics and Autonomous Systems*, 10(2): p. 199-205, 1992.

- 22] Singer, N., W. Singhose, and E. Kriikku, "An Input Shaping Controller Enabling Cranes to Move Without Sway," *ANS 7th Topical Meeting on Robotics and Remote Systems*, Augusta, GA, 1997.
- 23] Kress, R.L., J.F. Jansen, and M.W. Noakes, "Experimental Implementation of a Robust Damped-Oscillation Control Algorithm on a Full Sized, Two-DOF, AC Induction Motor- Driven Crane," *5th ISRAM*, Maui, HA, pp. 585-92, 1994.
- 24] Butler, H., Honderd, G., Van Amerongen, J., "Model reference adaptive control of a gantry crane scale model", *Control Systems Magazine*, IEEE Volume: 11 Issue: 1, Jan, 1991 Page(s): 57 -62.
- 25] Forest, C., Frakes, D., Singhose, W., "Input-Shaped Control of Gantry Cranes: Simulation and Curriculum Development", *Proceedings of the Eighteenth ASME Biennial Conference on Mechanical Vibration and Noise*, Sept. 2001.
- 26] Kenison, M., Singhose, W., "Input Shaper Design for Double- Pendulum Planar Gantry Cranes", *Proceedings of the IEEE International Conference on Control Applications*, 22-27 Aug. 1999 vol. 1, pp. 539 -544.

APPENDIX A

Coding MATLAB based on PZS, PZSD and PZSDD

i) Positive Zero Sway (PZS)

```

starting_time=0;
simulation_time=10;
sampling_time=0.001;
t=starting_time:sampling_time:simulation_time;

for i=1:(0.2/sampling_time)+1
    u(i,1)=1;
end
for i=(0.2/sampling_time)+1:(0.5/sampling_time)+1
    u(i,1)=2;
end
for i=(0.5/sampling_time)+1:(0.8/sampling_time)+1
    u(i,1)=0;
end
for i=(0.8/sampling_time)+1:(10/sampling_time)+1
    u(i,1)=1;
end

% Positive ZV shaper (2-impulse)
% mode 1
pi=22/7;
z1=0.0086;
k1=exp((-z1*pi)/((1-z1^2)^0.5));
wn1=6.78;
wd1=wn1*(sqrt(1-z1^2));

%Determine the amplitudes and time location of the input shaper
ip=2;
tt1a(1)=0;
tt1a(2)=pi/wd1;
A1a(1)=1/(1+k1);
A1a(2)=A1a(1)*k1;

tt1a=tt1a./0.001;

```

```

tt1a=round(tt1a);
tt1a=tt1a.*0.001;

for i=1
    v1a(i,1)=A1a(1);
end

ni=1;
while ni<=ip-1
    for i=((tt1a(ni)/sampling_time)+2):((tt1a(ni+1)/sampling_time)+1)
        v1a(i,1)=0;
    end
    for i=(tt1a(ni+1)/sampling_time)+1
        v1a(i,1)=A1a(ni+1);
    end
    ni=ni+1;
end

for i=((tt1a(ni)/sampling_time)+2):((30/sampling_time)+1)
    v1a(i,1)=0;
end

imp1a=v1a;
impa=imp1a(1:(10/sampling_time)+1);

shp1a=conv(impa,u);
PZS=shp1a(1:(10/sampling_time)+1);

```

ii) Positive Zero Sway Derivative (PZSD)

```

starting_time=0;
simulation_time=10;
sampling_time=0.001;
t=starting_time:sampling_time:simulation_time;

for i=1:(0.2/sampling_time)+1
    u(i,1)=1;
end
for i=(0.2/sampling_time)+1:(0.5/sampling_time)+1
    u(i,1)=2;
end
for i=(0.5/sampling_time)+1:(0.8/sampling_time)+1
    u(i,1)=0;
end
for i=(0.8/sampling_time)+1:(10/sampling_time)+1
    u(i,1)=1;
end

% Positive ZSD shaper (3-impulse)
pi=22/7;
z1=0.0086;
k1=exp((-z1*pi)/((1-z1^2)^0.5));
wn1=6.78;
wd1=wn1*(sqrt(1-z1^2));

%Determine the amplitudes and time location of the input shaper
ip=3;
t1b(1)=0;
t1b(2)=pi/wd1;
t1b(3)=2.*t1b(2);
A1b(1)=1/(1+2.*k1+k1.^2);
A1b(2)=A1b(1)*2*k1;
A1b(3)=A1b(1)*k1.^2;

```

```
tt1b=tt1b./0.001;
tt1b=round(tt1b);
tt1b=tt1b.*0.001;

for i=1
    v1b(i,1)=A1b(1);
end

ni=1;
while ni<=ip-1
    for i=((tt1b(ni)/sampling_time)+2):((tt1b(ni+1)/sampling_time)+1)
        v1b(i,1)=0;
    end
    for i=(tt1b(ni+1)/sampling_time)+1
        v1b(i,1)=A1b(ni+1);
    end
    ni=ni+1;
end

for i=((tt1b(ni)/sampling_time)+2):((30/sampling_time)+1)
    v1b(i,1)=0;
end

imp1b=v1b;
impb=imp1b(1:(10/sampling_time)+1);
shp1b=conv(impb,u);
PZSD=shp1b(1:(10/sampling_time)+1);
```

iii) Positive Zero Sway Derivative-Derivative (PZSDD)

```

starting_time=0;
simulation_time=10;
sampling_time=0.001;
t=starting_time:sampling_time:simulation_time;

for i=1:(0.2/sampling_time)+1
    u(i,1)=1;
end
for i=(0.2/sampling_time)+1:(0.5/sampling_time)+1
    u(i,1)=2;
end
for i=(0.5/sampling_time)+1:(0.8/sampling_time)+1
    u(i,1)=0;
end

% Positive ZSDD shaper (4-impulse)

pi=22/7;
z1=0.0086;
k1=exp((-z1*pi)/((1-z1^2)^0.5));
wn1=6.78;
wd1=wn1*(sqrt(1-z1^2));

%Determine the amplitudes and time location of the input shaper

ip=4;

ttlc(1)=0;
ttlc(2)=pi/wd1;
ttlc(3)=2.*ttlc(2);
ttlc(4)=3*ttlc(2);

```

```

A1c(1)=1/(1+3.*k1+3*k1.^2+k1^3);
A1c(2)=A1c(1)*3*k1;
A1c(3)=A1c(2)*k1;
A1c(4)=A1c(1)*k1^3;

```

```

tt1c=tt1c./0.001;
tt1c=round(tt1c);
tt1c=tt1c.*0.001;

```

```

for i=1
    v1c(i,1)=A1c(1);
end

```

```

ni=1;
while ni<=ip-1
    for i=((tt1c(ni)/sampling_time)+2):((tt1c(ni+1)/sampling_time)+1)
        v1c(i,1)=0;
    end
    for i=(tt1c(ni+1)/sampling_time)+1
        v1c(i,1)=A1c(ni+1);
    end
    ni=ni+1;
end

```

```

for i=((tt1c(ni)/sampling_time)+2):((30/sampling_time)+1)
    v1c(i,1)=0;
end

```

```

imp1c=v1c;
impc=imp1c(1:(10/sampling_time)+1);

```

```

shp1c=conv(impc,u);
PZSDD=shp1c(1:(10/sampling_time)+1);

```